

Published: June 30, 2023

Citation: Muñoz A and Oliviero A, 2023. Cerebrospinal CNS-Leaks: State of the Art in Imaging Diagnosis with Special Focus on Intrathecal MRI Paramagnetic Contrast Agents Procedures, Medical Research Archives, [online] 11(6). <https://doi.org/10.18103/mra.v11i6.3844>

Copyright: © 2023 European Society of Medicine. This is an open-access article distributed under the terms of the Creative Commons Attribution License, which permits unrestricted use, distribution, and reproduction in any medium, provided the original author and source are credited. DOI <https://doi.org/10.18103/mra.v11i6.3844>

ISSN: 2375-1924

RESEARCH ARTICLE

Cerebrospinal CNS-Leaks: State of the Art in Imaging Diagnosis with Special Focus on Intrathecal MRI Paramagnetic Contrast Agents Procedures

Alberto Muñoz*¹, Antonio Oliviero²

1. Department of Radiology. School of Medicine. Universidad Complutense de Madrid. 28040. Madrid. Spain
2. FENNSI Group, Hospital Nacional de Parapléjicos (SESCAM), Toledo (Spain) y Center for Clinical Neuroscience, Hospital Los Madroños, Madrid, Spain.

* almugo7557@gmail.com

ABSTRACT

MR imaging has proved invaluable in anatomic depiction of the cerebrospinal fluid (CSF) spaces and the surrounding neural and non-neural tissue, although there are still some clinical situations (i.e., cases of CSF-flow alterations, communicating or non-communicating cyst masses bordering CSF pathways, or craniospinal CSF leaks) in which further imaging tests may be required for a definitive diagnosis.

This paper will review the state-of-the-art imaging in these processes, including Radionuclide Cisternography, plain Computed Tomography (CT) and enhanced-CT Cisternography/ myelography, as well as Magnetic Resonance Imaging (MRI) and contrast-enhanced Cisternography/myelography, emphasizing the latest CT and MR imaging refinement advances and proposing tailored specific approaches for two well-established clinical syndromes, namely CSF rhinorrhea and intracranial hypotension syndrome.

Key words: CSF leak imaging; CSF rhinorrhea imaging; Spontaneous rhinorrhea and otorrhea; CSF otorrhea imaging; Radioisotope cisternography; Intrathecal Gd enhancement; MR cisternography; Intracranial hypotension imaging.

Abbreviations

AS: Aqueductal Stenosis
CE-CTC: Contrast-enhanced CT-Cisternography
CE-CTM: Contrast-enhanced CT-Myelography
CE-MRC: Contrast-enhanced MR-Cysternography
CE-MRM: Contrast-enhanced MR-Myelography
CSF: Cerebrospinal Fluid
CT: Computed tomography
CVF: CSF-venous fistula
DCTM: Dynamic CT-myelography
DFM: Dynamic fluoroscopic myelography
DSM: Digital Subtraction Myelography
EBP: Epidural blood patch
Gd: Gadolinium
GBCA: Gadolinium-based contrast agents
HRCT: High-Resolution CT
IH: idiopathic intracranial hypertension
iv: intravenous
LP: Lumbar Puncture
NCHRT2W-MRC: Non-contrast High-Resolution T2-weighted MR-cisternography
NCHRT2W-MRM: Non-contrast High-Resolution T2-weighted MR-myelography
NC-MRC: Non-contrast MR cisternography
MRI: Magnetic Resonance Imaging
PPH: Postdural Puncture Headache
RC: Radioisotope Cisternography
SIH: spontaneous intracranial hypotension
SLEC: spinal longitudinal extradural CSF collection

INTRODUCTION

Computed Tomography (CT) and Magnetic Resonance Imaging (MR) are currently the preferred techniques for the diagnosis of morphological diseases involving the CNS. Intravenous contrast materials may add important information, particularly regarding abnormalities in blood-brain-barrier integrity which is frequently disturbed by neoplastic and inflammatory illness. MRI is superior to CT in depicting many lesions. Advantages of MRI over CT relies on its superior contrast resolution, superb anatomic display, and absence of radiation exposure. For these reasons MRI is the standard of imaging reference in processes involving the brain and spinal cord.

MRI has also proved invaluable in the anatomic depiction of the cerebrospinal fluid (CSF) containing spaces surrounding neural and non-neural tissues. However, there are still some clinical situations (i.e., cases of CSF flow alterations, communicating or non-communicating cyst masses bordering CSF pathways, or craniospinal CSF leaks) which may require further imaging tests for definitive diagnosis and there are still a number of conditions where CSF contrast enhancement is beneficial, including assessment of the subarachnoid spaces, abnormal CSF collections and leaks, or as a

mean to study CSF dynamics. Both radioisotope cisternography (RC) and CT with intrathecal water-soluble iodinated contrast media have been used for this purpose but have limitations and use ionizing radiation¹⁻⁴.

Cisternography is defined as imaging of the cerebrospinal system and associated structures after intrathecal administration of contrast material into the subarachnoid space^{5,6}. Cisternographic studies have been in use for at least 50 years for the evaluation of abnormalities of the intracranial CSF-filled spaces, cranium base, and vertebral column. Cisternography is called "myelography" if it is dedicated to the spinal canal^{5,6}. In this review, different imaging techniques performed after intrathecal contrast agent administration will be called indistinctly "cisternography." Ventriculography relies on the imaging of the ventricular system after the intraventricular injection of contrast material whether isotopic, iodinated, or paramagnetic.

The main limitations of RC are lack of cross-sectional images and lower spatial resolution. CT has overcome these limitations; however, both contrast-enhanced CT cisternography (CE-CTC) and RC involve radiation exposure, which is a more important factor to consider because cisternographic studies often require consecutive or multiple acquisitions⁵⁻¹⁰.

Non-contrast High-Resolution T2-weighted MR Cisternography/Myelography (NCHRT2W-MRC) derived from heavily 3D T2-weighted MR sequences (such as fast imaging with steady state acquisition, CISS, FIESTA, or sampling perfection with application optimized contrast using different flip angle evolutions) has been developed to overcome the above-mentioned limitations of CE-CTC/M and RC¹¹⁻¹⁴. High contrast-to-noise ratio, multiplanar evaluation of volumetric data, and thin-section image acquisition are the main advantages of NCHRT2W-MRC⁵. Moreover, it is non-invasive, and it does not require radiation exposure or intrathecal contrast material administration⁹. Although NCHRT2W-MRC has several advantages, it can only provide morphologic information different from that in other cisternographic studies^{15,16}.

Contrast-enhanced MR cisternography/myelography (CE-MRC) can provide both physiologic and morphologic information¹⁰ and it is a less invasive technique compared with other cisternographic and ventriculographic (RC or CE-CTC) tests, enabling of all the advantages of MR imaging¹⁵.

This paper will review the imaging diagnosis techniques and a comprehensive, state of the art comparison of the latest radiological advances and refinements, as well as a practical

clinical approach in the two most important clinical CSF flow alterations: CSF rhinorrhea and intracranial hypotension syndrome.

METHODS & RESULTS

A comprehensive search in accordance with PRISMA guidelines (Preferred Reporting Items for Systematic Reviews and Meta-Analyses) using search terms of interest was completed through PubMed, Scopus, and reference lists from relevant articles to identify literature on sensitivities and accuracies of different imaging methods for localization and detection of CSF leaks. Search terms included were “CSF leak imaging”, “CSF rhinorrhea imaging”, “spontaneous rhinorrhea and otorrhea”, “CSF otorrhea imaging”, “radioisotope cisternography”, “intrathecal Gd enhancement”, “MR cisternography”, and “intracranial hypotension imaging”. These studies included meta-analyses, original prospective and retrospective papers, case reports, and others (technical notes, appraisals, commentaries, or editorials) published from 1995 until present. Reference lists of these articles and ongoing investigations in this area were also included. All papers had a Level of Evidence of 2 or 3, as no studies with higher Level of Evidence, such as randomized controlled trials, were identified.

A total of 857 papers were selected: CSF leaks, 661; IHS, 95; MR cisternography, 47; spontaneous rhinorrhea and otorrhea, 18; RC, 12; intrathecal Gd enhancement, 24. From these, only 143 were considered valid for the purpose of the revision. Meta-Analyses studies were 4; prospective studies were 16; retrospectives 25; short case series and case reports 41; reviews 31, and others 26.

RATIONALE AND BASIS FOR THE USE OF INTRATECHAL PARAMAGNETIC CONTRAST

Underlying mechanism of CSF enhancement by Gadolinium (Gd) on T1-weighted MR images rely on shortening the relaxation time of the water when a diluted paramagnetic contrast agent interacts with neighboring water protons (proton relaxation enhancement effect)¹⁷⁻²¹. At lower concentrations of Gd, the main effect is on T1, while at higher concentrations the main effect is on T2, and paradoxical phenomena may appear on T1 (Fig. 1). The lower dosage of diluted Gd used (0.2-5 mL) is adequate for diagnostic subarachnoid enhancement on MRI in most clinical situations²¹⁻²³. At these doses, CE-MRC provides excellent contrast and anatomic depiction of CSF-containing spaces and surrounding tissues.

Figure 1. Imaging of mechanism of CSF enhancement by Gd on T1-weighted images due to shortening the relaxation time of the water when different concentration of paramagnetic contrast agent are diluted, and subsequent paradoxical phenomena. Axial T1-weighted image after intracavitary Gd injection show giant cyst-like appearance of a craniopharyngioma with a supernatant hyperintense content and absence of signal in the subnatant gravitation-dependent fluid level. This is due to the paradoxical low signal caused by increased contrast concentration.

(Reproduced from Muñoz A et al⁷⁷ with permission).



ETHICAL AND LEGAL QUESTIONS. SAFETY AND HAZARD CONSIDERATIONS

The safety of intrathecal GBCA have been reported in several pilot studies in Europe^{6,9,10,24,25}. Tolerance and dose limits of intrathecal Gd injection were established in animal model studies, and different Gd compounds or gadolinium-based contrast agents (GBCA) were compared in different experimental animal protocols²⁶⁻²⁸ on both animals and humans. Its safety and tolerance have been well established in clinical trials in rhinorrhea/otorrhea and spinal CSF leaks, with a the low incidence of side effects^{6,8,10,21-26,28-33}. Furthermore, CE-MRC seems to have a higher sensitivity in detecting pathology than their CE-CT corresponding procedures^{23,34-37}.

Animal studies have demonstrated that a high dose of intrathecal GBCAs, such as gadopentetate dimeglumine and gadodiamide, can result in signs of neurotoxicity such as gait disturbance, myoclonus, ataxia, tremors, and seizures³⁷⁻³⁹ both in animals and humans. These adverse events occur at doses equivalent to 5–15

μmol per gram of brain tissue and are associated with histopathologic findings, including loss of oligodendroglia, astrocytic hypertrophy, and eosinophilia³⁸⁻⁴⁰. Some case reports in humans have shown evidence of neurotoxicity after intrathecal injection^{28,41-43}. Most of these cases involved accidental overdoses, which resulted in signs and symptoms such as confusion, global aphasia, vomiting, stupor, rigidity, seizures, and hypertension^{44,45}. It was concluded that these changes and disturbance did not occur if the total injected dose was 15 mL (3.3 mmol/g)³⁷⁻⁴⁴. Direct intraventricular injection of Gd has been subject to trials only in animal models. In humans, only 3 patients had an inadvertent direct intraventricular high dose injection of Gd-DTPA, and in one of the patients with fatal outcome⁴³.

Intrathecal use of GBCAs is not currently approved in many countries and it is not approved by the FDA in the US or EMA in the UE. Therefore, the clinical use of intrathecal/intraventricular GBCA are restricted to specific clinical scenarios and always performed when judged to be a better or the only alternative.

Health Systems organizations in some countries require that physicians opt for the so-called merciful use of drugs. That means that the team of doctors responsible for the care of a patient may use a drug that has been approved for other conditions as long as it is prescribed on an individual basis, the patient is never enrolled in a clinical trial, and he/she acknowledges after being informed that drug is not officially approved for the proposed study. Moreover, multiple other relative contraindications exist to performing contrast intrathecal injections, which must be taken into consideration before carry out any study such as RC, CE-CTC, or CE-MR. In particular, these include a history of seizures, a grossly bloody spinal tap, hematoma or infection at the puncture site, pregnancy, space-occupying intracranial process with increased intracranial pressure, evidence of bleeding disorder or coagulopathy, myelography performed within 1 week, previous surgical procedure in anticipated puncture site, generalized septicemia, and a history of allergy or intolerance to iodinated contrast media and/or gadolinium-based MR contrast agents. Complications of intrathecal injection include postprocedural headache, infection, and minor bleeding⁴⁵.

The literature review was unable to identify any randomized controlled trials of GBCA, because of its off-label use, and all studies were observational with no control groups. Furthermore, because of the ethical constraints associated with administration of an off-label substance, it would

be difficult to conduct randomized controlled trials to assess intrathecal GBCAs safety. According to the largest meta-analysis conducted, Patel et al⁴⁶ reviewed 33 studies, none of them randomized controlled trials, that included a total of 1036 patients who had received intrathecal GBCAs, the overall rate of reported adverse events was 13%; although the rate of serious adverse events was not amenable to meta-analysis, serious events were noted in 10 patients. The authors concluded that intrathecal administration of GBCAs were not associated with serious neurotoxic adverse effects at doses lower than 1.0 mmol. The most commonly reported adverse effect associated with intrathecal injection of GBCA was a transient postural headache lasting less than 24 hours, occurring in 13% of cases, that could be confounded for postural headaches commonly seen after LP procedures, with a reported incidence of up to 49% in the literature^{47,48}, the discrepancy between the incidence of postural headaches in our analysis and the literature is likely due to an underreporting of minor symptoms associated with lumbar puncture given that adverse events after intrathecal administration of GBCAs was not the primary focus for most studies⁴⁶. Few patients reported nausea, emesis, or fever. Serious adverse events reported in 10 patients included various symptoms relating to neurotoxicity, including "...seizures, dysarthria, ataxia, confusion, visual disturbances, vertigo, myoclonic jerks, aphasia, changes in extremity muscle tone, and mental status changes,"⁴⁶. The authors also found a strongly statistically association between the seriousness of the adverse event and the dose of the intrathecally administered GBCAs. All minor adverse events were reported in patients who had received 1 mmol or less of GBCA intrathecally (most were 0.25 or 0.5 mmol), whereas the intrathecal dose for all reported serious adverse events was 2 mmol or greater (range, 2–10 mmol)⁴⁶. All serious adverse events, but one, occurred acutely, with nine of 10 studies reporting adverse events within the first 6 hours after intrathecal GBCA exposure⁴⁶.

Although not strictly an adverse event, it is consider the issue of increased central nervous system gadolinium chelates deposition within the human brain extravascular space after repeated intravenous administrations⁴⁶. In this issue, GBCA can be classified into linear and macrocyclic agents. Macrocyclic agents, such as gadobutrol, are more recent agents developed to decrease the potential side effects of GBCA^{46,49-51}. There are several reports searching for the MRI brain changes and effects of the intrathecal injection of linear GBCA^{52,53}. In term of CNS chronic agents deposition the new macrocyclic agents have proved not to

show these effects previously reported with linear agents, although its toxicity are also dose-dependent⁴⁶. In particular with this regard, there are two prospective studies searching for the side clinical effects and CNS contrast deposition of gadobutrol at a dose of 0.5 mmol, which concluded that its intrathecal administration in doses of either 0.25 or 0.5 mmol was safe and without serious effects^{54,55} and that intrathecal macrocyclic GBCA administration was not associated with measurable T1 signal intensity changes in the globus pallidus and dentate nuclei, as an indicator of brain gadolinium deposition detectable by MRI⁵². For these reasons, currently there is a trend towards change in GBCA administration from the linear ones to the macrocyclic, not only in its intrathecal use but also in any administration route.

CURRENT MAIN INDICATIONS OF GADOLINIUM-ENHANCED MRI CISTERNOGRAPHY/MYELOGRAPHY

1. CRANIAL CSF LEAKS (CSF-RHINORRHEA AND OTORRHEA)

CSF leaks are extracranial egress of CSF into the adjacent paranasal sinus (rhinorrhea) or tympanomastoid cavity (otorrhea) due to an osteo dural defect involving skull base³². CSF fistulas can be classified as traumatic/postsurgical, spontaneous, or iatrogenic according to etiology. Traumatic cases are the commonest occurring in up to 30%^{56,57} and up to 30% of skull base surgeries⁵⁸. The most common sites were ethmoid roof, cribriform plate, and sphenoid sinus³⁵. Traumatic CSF leaks often close spontaneously and may be treated conservatively. However, if persistent, the CSF leakage site may be a port of entry for bacteria, causing meningitis or other complications, and may need surgical repair⁵⁹. Precise localization of the fistula before surgery increases the rate of successful repair and decreases the duration of the operative procedure. Although many non-radiologic tests and ancillary procedures may help to refine the diagnosis in patients who required surgical treatment, a definitive diagnosis depends on demonstration of the fistula site by imaging procedures. CSF leaks may also occur in patients without any known precipitating factor, so called spontaneous CSF leaks, comprising up to 40% of a CSF case series⁶⁰. Spontaneous leaks are an increasing recognizable cause of CSF-leaks seen in obese, middle-aged women with sleep apnea and orthostatic headaches, who present with clinical features and imaging findings of increased intracranial pressure, similarly as those seen in patients with idiopathic intracranial hypertension (IIH), normal CSF, and without imaging evidence of

mass lesion or hydrocephalus⁶¹. Typical MR imaging findings include prominence of perioptic CSF spaces, posterior scleral flattening or protrusion of optic nerve head, prominent arachnoid granulations causing skull base erosions, empty sella and meningoencephalocele³². Ancillary radiologic findings associated with IIH include bilateral transverse sinus stenosis and low-lying cerebellar tonsils along with inferiorly displaced brainstem and cerebellum as in Chiari 1 malformation⁶². The proposed mechanism for the development of meningoencephalocele and spontaneous leaks in IIH is due to impaired CSF absorption by arachnoid granulations causing fluctuating or persistent elevation in intracranial pressure leading to bony erosions which can facilitate herniation of meninges and brain tissue through the areas of least resistance¹⁰. There are also CSF leaks caused by congenital or acquired breaches of the osteodural barrier (congenital encephaloceles, primary empty sella syndrome, Stenberg's canal, tumor erosion, etc.), that are often included within the spontaneous CSF leak group, and whose incidence has not been properly established⁶³.

CSF-otorrhea is a particular form of base of the skull leaks resulting from abnormal communications between subarachnoid spaces and pneumatized parts of the temporal bone and sinonasal tract through osteo dural defects at the base of the skull^{32,56} and could be associated with rhinorrhea because CSF may leak through the Eustachian tube into the nasopharynx/nasal cavity⁶⁴. The presence of temporal bone fracture along with air pockets in inner ear structures, including vestibule and semicircular canals, help to direct the imaging procedure workup.

Identification of glucose in nasal or ear secretions has been widely reported for the identification of CSF, given its availability, cost, and ease to perform. However, its sensitivity and specificity are low, since hyperglycemia, epithelial inflammation, bacterial infection or contamination with nasal mucus, blood and tears may alter its result⁶⁵. Zapalac et al⁶⁶ proposed a diagnostic algorithm for skull base CSF leaks in 2002 involving confirmation with beta-2 transferrin and that should always be measured before any invasive procedure, so that excluding non specific causes of rhino-otorrhea.

The initial imaging techniques that can be used for preoperative assessment of the patients to determine the CSF-fistula site are firstly non-invasive, including high-resolution computed tomography (HRCT) and non-contrast enhanced MR cisternography (NCE-MRC). Imaging mini-invasive studies including RC, CE-CTC, and CE-MRC are utilized in selected cases. The choice of the imaging

modality and its diagnostic accuracy depends on the local experience and expertise along with technical capabilities of the modality.

Radioisotope Cisternography

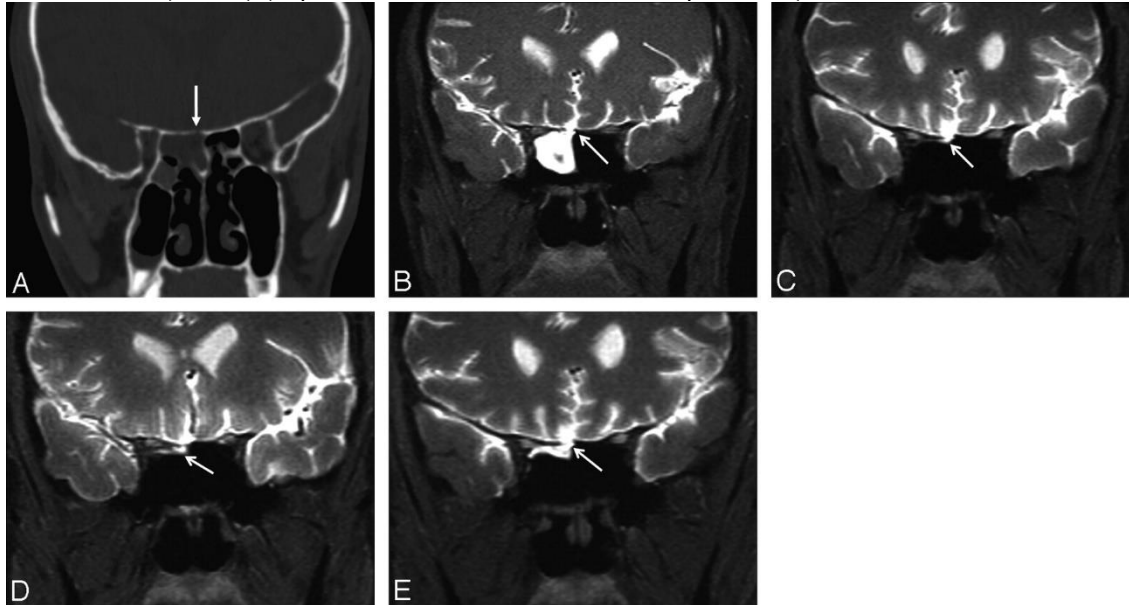
The technique consists of intrathecal injection of radiopharmaceutical radiotracers, either technetium (^{99m}Tc)- or indium (^{111}In)-labeled Diethylenetriamine pentaacetic acid (DTPA), with periodic imaging. Usually acquisition of the images as standard protocol consists on imaging at 1, 2, 4, 24, and 48 hours postinjection. Imaging at multiple time points aids in the detection of intermittent or slow leaks⁴⁵. Detection of the radiotracer activity in the sinonasal cavity or the nasopharynx indicates a positive study. However, RC is no longer an imaging procedure in the detection of the base of the skull CSF fistula and it is rarely performed now-a-days for the following reasons. First, active CSF leakage should be present at the time of study for accurate diagnosis. Second, intermittent CSF leaks are poorly demonstrated by Tc- 99m radionuclide study, although a prolonged cisternography could be performed with a radiotracer having a longer biological half-life such as the Indium 111 diethylenetriamine pentaacetic acid and delayed imaging could be performed with this radionuclide for up to 72 h for diagnosis of intermittent CSF leak¹. Third, the accuracy of RC is reported to be 70% in active leaks and much lower (i.e., about 28%, in inactive leaks, low-flow fistula or hairlike communications)^{9,10,40}. Other disadvantages are the same as with CE-CTC, including mini-invasive nature and radiation

exposure. Moreover, routine use of RC alone or in conjunction with CT increases the radiation exposure significantly. Currently, RC is being used as an alternative modality, primarily in cases with intermittent leaks to confirm presence or absence of a CSF leak⁶⁴.

Computed Tomography

Non-contrast HRCT of the base of the skull, specifically paranasal sinuses and the temporal bones, is usually the first line of image performed in patients with CSF leaks⁶⁷. Nowadays multidetector CT scanners acquire isotropic, volumetric, thin submillimetre bone algorithm sections, allowing multiplanar reformations with excellent delineation of bony anatomy with unparalleled identification of any bony defect. The images can also be used for intraoperative navigation along with endoscopic views. Shortcomings of HRCT are insufficient demonstration of the concomitant dural defect and to distinguish mucus secretions from the CSF collection within the air cells adjacent to normal areas of bony thinning/dehiscence in the skull base⁶⁸, particularly in postoperative or posttraumatic states since high attenuation bone fragments, bone artifacts and anatomic bone detail makes the images difficult to evaluate, and at times inconclusive (fig. 2). Overall, the sensitivity of HRCT for CSF leaks varies between 84–95% with specificity between 57–100%^{69,70}. Identification of a single defect in a patient with a positive correlation between the location of the bony defect and clinical symptoms obviates the need for further imaging.

Fig. 2 (A-E). CSF rhinorrhea following head trauma in a 35-year-old man. A, coronal thin-section CT scan reveals a defect in the roof of the sphenoid sinus (arrow) and opacification of the right sphenoid sinus. B, A coronal T1-weighted fat-saturated MR cisternogram obtained after the intrathecal administration of Gd-DTPA shows contrast leakage (arrow) extending from the cranial subarachnoid space into the right sphenoid sinus. C, after repair of the dural rupture, suspected CSF rhinorrhea recurred 1 week later and the patient underwent control MR cisternography. Images obtained in the first hour show probable leakage (arrow). D and E, Leakage becomes obvious in late images taken in the third and fifth hours (arrows). (Reproduced from Selcuk H et al¹⁰ with permission).



Non-contrast enhanced MR cisternography (NCE-MRC)

The principle of NCE-MRC cisternography is to demonstrate a contiguous fluid signal between the cisternal space and nasal sinus on heavily weighted T2 images. Hence, imaging during prone position is recommended. NCE-MRC exploits the relative high signal intensity of the CSF in subarachnoid spaces using heavily T2-weighted sequences with suppression of background signal from the soft tissue and cerebral parenchyma. The major disadvantage is the lack of bony detail. When positive, NC-MRC leakage is characterized by a hyperintense tract between the subarachnoid space and the sinonasal spaces^{32,71}. Submillimeter acquisition and multiplanar reformats facilitate optimal evaluation of the skull base defects⁷². The reported sensitivity of NCE-MRC in the detection of a CSF leak is about 94%⁷³. Due to excellent soft

tissue resolution, NC-MRC facilitates delineation of contents herniating through the bony defect and differentiates meningocele from an encephalocele with adjacent gliotic parenchyma⁷⁴. NCE-MRC yields higher accuracy than HRCT for non-invasive diagnosis and localization of CSF fistula. As a result, NCE-MRC can be chosen as a first-line imaging technique because there is no ionizing radiation exposure or contrast medium administration, and this technique is non-invasive and has a high soft-tissue contrast without artifacts from bony elements³⁵. However, in surgical cases non-contrast MR cisternography must be interpreted along with HRCT as MR imaging fails to provide optimal bony detail^{74,75}. In more complicated situations such as in patients with positive results on a beta 2-transferrin test but no visualized CSF leak or suspicious leak on NCE-MRC, CE-MRC should be performed (fig. 3).

Fig 3 (A-C). Example of false positive NC-MRC and true positive CE-MRC. Coronal T2WI (A), coronal intrathecally CE-MR (B), and axial intrathecally CE-MR fat-suppressed T1 WI (C) of a 52-year-old man with suspected CSF rhinorrhea. NC-MRC falsely depicts a possible leakage at the frontal sinus roof (white arrow head), whereas CE-MRC correctly points to a surgery proven left ethmoid region defect (white arrows). (Reproduced from Ecin G et al⁷¹ with permission).



Contrast-enhanced CT cisternography

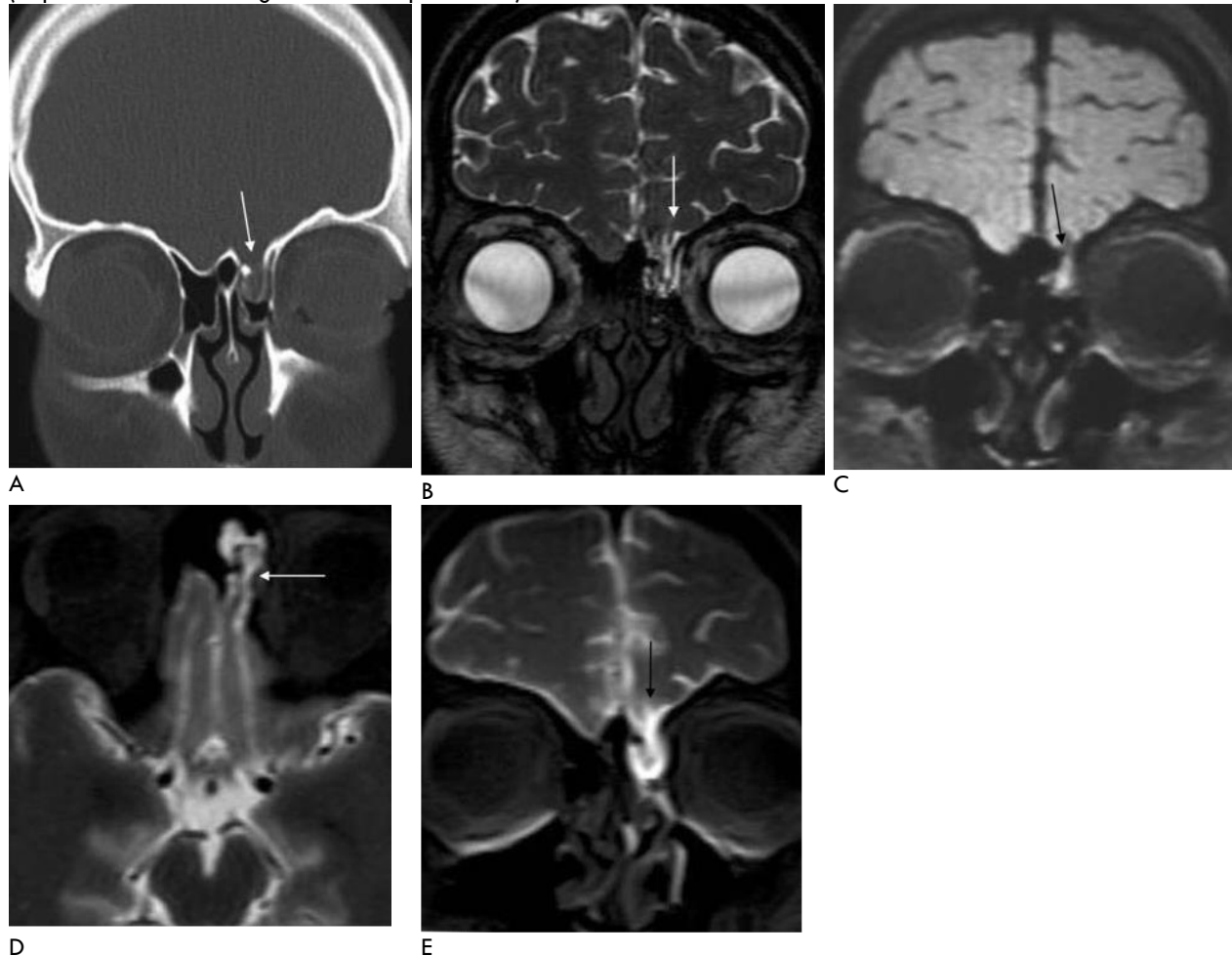
CE-CTC only elicits the site of leak in active cases and should be compared with HRCT done prior to contrast instillation for optimal evaluation of contrast leak. The main indication of CE-CTC is to assess CSF leaks in patients with multiple fractures and osseous defects, and those with a suspicious bony defect and clinically confirmed leaks³². A positive study is considered when there is contrast pooling throughout and down back to a bony defect⁶⁹. The sensitivity of CE-CTC ranges between 85–92% in patients with active leak and 40% in those with inactive leak⁷⁰.

The main shortcomings of this technique are the low sensitivity in patients with inactive/intermittent leaks and obscuration of small leak due to non-leakage of high viscosity contrast, adjacent to high-density bone^{70,74} (Fig. 4). Also, drawbacks of the CE-CTC procedure includes its mini-invasive nature, increased radiation dose due to multiple scans, inherent risks associated with a lumbar puncture and intrathecal instillation of iodinated contrast.

Fig 4. Spontaneous rhinorrhea, which turned out to be secondary to a base of the skull defect, whose CE-CTC was negative. Midsagittal T1-weighted fat-suppressed CE-MRC through the base of the skull shows contrast leakage in the sphenoidal sinus (arrow).



Fig. 5 (A-E). An 18-year-old man with recurrent meningitis after trauma. A, coronal high-resolution CT image demonstrates the bone defect in the left cribriform plate (arrow). B, Cerebrospinal fluid (CSF) leak from the left cribriform plate is nicely seen on the coronal three-dimensional constructive interference in steady state (3D-CISS) image (arrow). The size and relationship of the defect with neighboring structures and CSF leak (arrows) is clearly depicted on non-enhanced coronal (B), axial (D), and coronal (E) contrast-enhanced MR cisternography (CE-MRC) images. (Reproduced from O. Algin et al⁹ with permission).



Contrast-enhanced MR cisternography

CSF leaks are the most common clinical condition for CE-MRC is performed, particularly in spontaneous or posttraumatic/postsurgical rhinorrhea, outperforming CE-CTC. The sensitivity ranges from 92–100% in patients with active leaks and about 70% in patients with inactive leaks with a reported specificity of 80%^{10,71}. Valsalva maneuvers just before postcontrast image acquisition can be helpful in localizing the leakage site.

The main advantages CE-MRC are detection of intermittent CSF leaks (fig. 2 and 5), which can be attributed to its ability to perform delayed imaging up to 24 hours⁷⁶, demonstration of low-flow fistula or hairlike communications, a depiction of meningoceles (fig. 6), and relative ease of assessment of leak compared to CE-CTC, attributable to the differentiation between the

hyperintense contrast and adjacent bone^{10,21,66,69}. State of the art imaging in this setting introduces the so called CS T1 SPACE sequence, which offers a global 3D view of the entire skull base, meninges, and brain with high spatial detail and a global 3D view⁷⁸ (fig. 7). This technique is particularly suitable as a problem-solving tool using macrocyclic GBCA in patients with high clinical suspicion of intermittent leaks. In cases of otorrhea CE-MRC has shown high promising (fig. 8). The single center longest CSF-otorrhea series, that involves 16 patients who underwent CE-MRC, reported an overall sensibility and specificity quite high and superior to HRCT (89.3 and 72%, respectively)³⁰. The main shortcoming of CE-MRC is the lack of US and EU legal approval for the intrathecal administration of GBCA.

Table 1 proposes a diagnostic algorithm for skull base CSF leaks.

Table 1: Diagnostic algorithm for skull base CSF leaks (Taken from Zapalac et al⁶⁶ with modifications). HRCT: high resolution Computed Tomography; PNS: paranasal sinus; CE-MRC: contrast-enhanced MR-cisternography; NCE-MRC: non-CE-MRC.

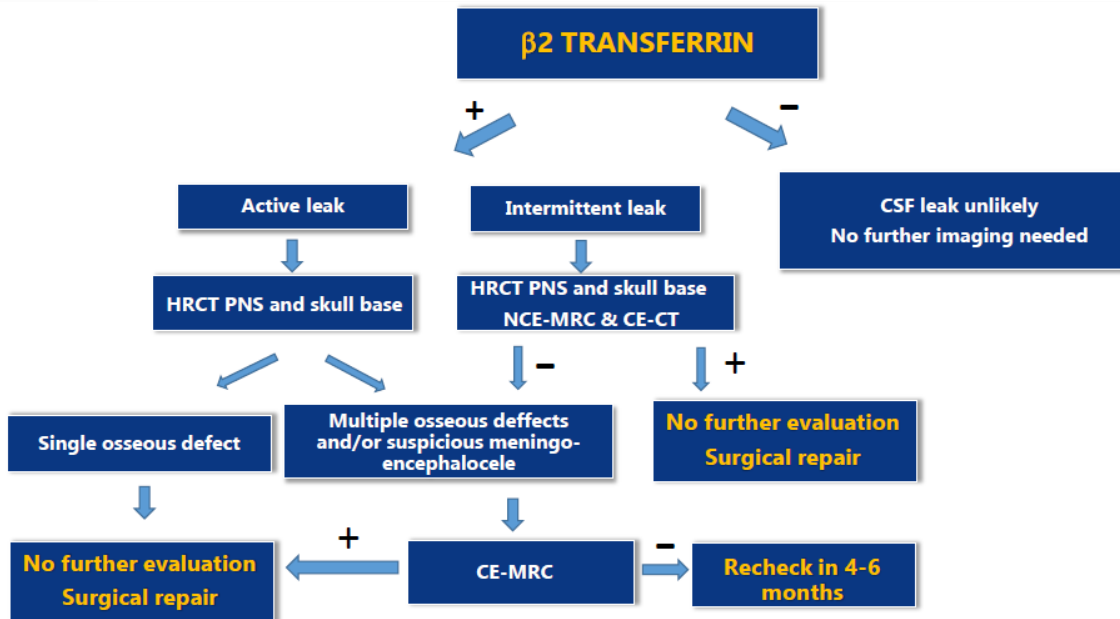


Fig. 6 (A-C). Example of full MRI demonstration of the pathologic contents in complex postsurgical states. MR imaging of a craniofacial malformation (Crouzon syndrome) after surgical fronto-orbital advance. Two months after the procedure the patient experienced intermittent rhinorrhea. Midsagittal CE-MRC image (A) before surgery shows cranial deformity and enlargement of ventricles. No base of the skull defects are seen. Midsagittal (B) and coronal (C) CE-MRC images at the level of the third ventricle and after intrathecal Gd injection demonstrates a CSF leak into the left nasoethmoidal (thin arrow) space and an acquired meningoencephalocele through the anterior base of the skull (thick arrow). (Reproduced from Muñoz A et al³¹ with permission).

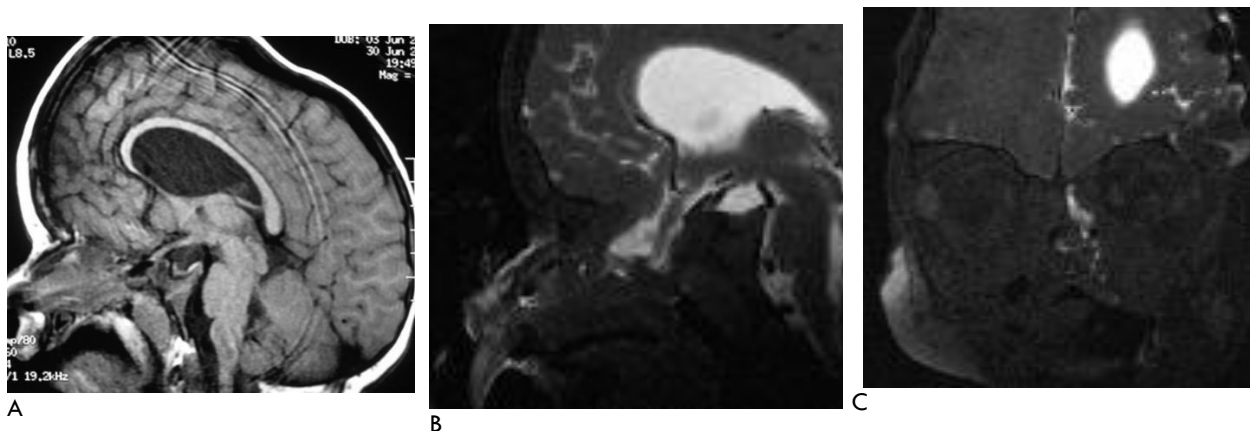


Fig. 7 (A-C). A 55-year-old woman (patient 1) who was readmitted for recurrent spontaneous left-sided CSF rhinorrhea and persistent slight headaches while sitting or standing after previous endoscopic sinus surgery. One year earlier, sealing of cribriform plate with TachoSil (Takeda Pharma) for suspected CSF leak had been performed. CT cisternography (soft tissue window level, W: 350; L: 50) is unremarkable, even in retrospect (A and B arrows). CS SPACE MR cisternography demonstrates a subtle CSF leak originating from the anterior rim of the left cribriform plate near foramen cecum (C and D, arrows) with a thin CSF collection extending to the anterior nasal cavity (arrowheads in C and E). The site correlated with the patient's intraoperative findings. After surgical repair, the patient was free of CSF rhinorrhea. (Reproduced from Duman IE, et al⁷⁸ with permission).

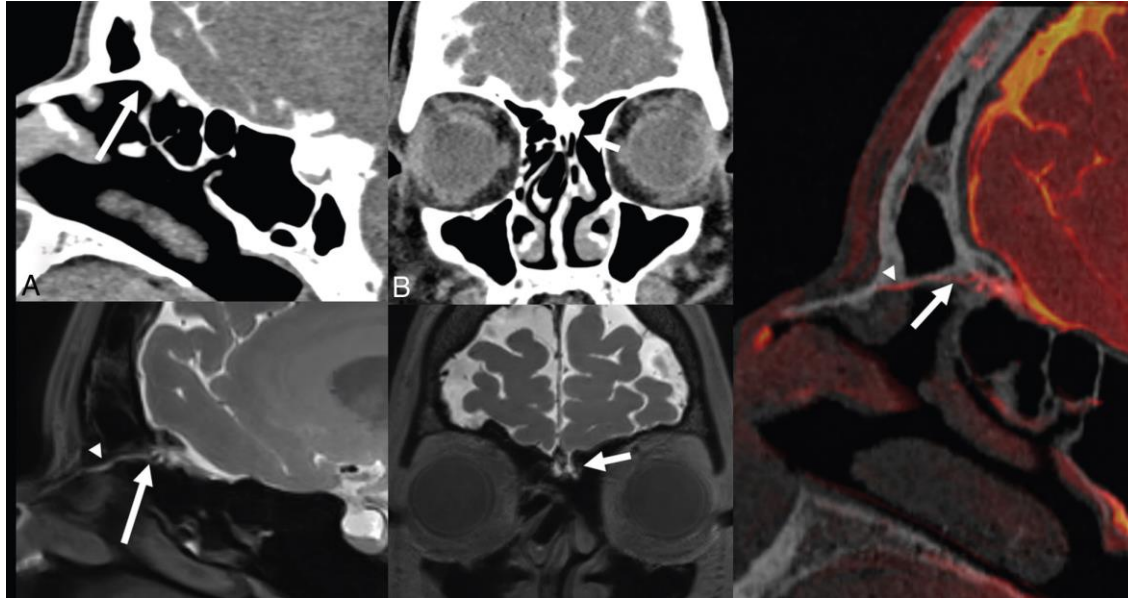
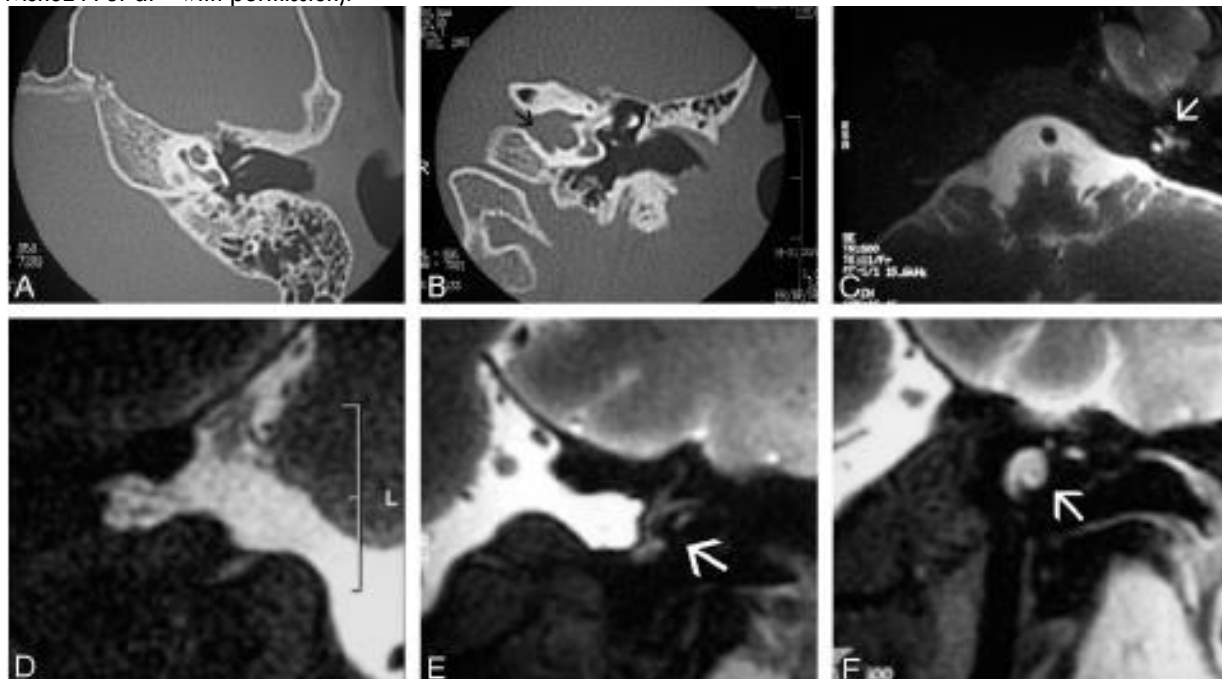


Fig. 8 (A-C). "Spontaneous" otorrhea and dizziness in a patient with CSF labyrinth fistula. A and B: axial and coronal CT scan through the left middle ear and osseous labyrinth show absence of osseous cochlear dysplasia (A) and bulbous appearance of the internal auditory canal (arrow in B) with no middle ear or mastoid cavity filling. C, T1-weighted fat-saturated CE-MRC image through the upper medulla oblongata shows abnormal filling of the left cochlear structure (arrow). D-F, T1-weighted fat-saturated CE-MRC images through the cerebellopontine cisterns. Axial (D) and spot view of the right side (E) show CSF filling up to the lamina cribrosa. However, further membranous labyrinth structures (semicircular canals) are filled on the left side (arrow in F) as well as cochlear duct (arrow in F). (Reproduced from Muñoz A et al³¹ with permission).



2. SPONTANEOUS INTRACRANIAL HYPOTENSION

SIH is caused by spinal CSF leaks, through small spinal dural tears, leaking meningeal diverticula, and CSF-venous fistulas, resulting in continued loss of CSF volume, leading to CSF hypovolemia, thus promoting multiple debilitating clinical manifestations⁷⁹. It is pathogenetically separated from that of LP, and from postoperative CSF loss⁸⁰. Also, CSF leaks due to penetrating dural injury from major traumatic events or iatrogenic cause are not considered to represent SIH and are classified separately⁸¹. Moreover, their clinical course and management differ.

The diagnosis of SIH remains difficult due to the various clinical manifestations, some of which are nonspecific and easily to be neglected^{81,82}. Major risk factors for SIH include disc degenerative diseases and underlying connective tissue disorder, such as Marfan syndrome or Ehlers-Danlos syndrome, hyperflexible joints neurofibromatosis, and Lehman syndrome, which predisposes to weakness of the spinal dura mater such as dura meningeal diverticula and dural tears⁸³. Besides, patients with these genetic connective tissue disorders, are at higher risk of spontaneous spinal CSF leaks than the general population^{84,85}.

For the purpose of this review from here on we will refer specifically to cases of spontaneous SIH. Differential diagnosis of SIH with other syndromes presenting with orthostatic headache is crucial, but it is beyond the scope of this review.

SIH can occur at any age, although most patients are middle-aged and there is a female preponderance (female: male ratio of 1.5: 1)⁸⁶ with an estimated annual incidence of 5/100,000⁸². Trauma, ranging from motor vehicle accidents to minor incidents such as sporting injuries, tumble, or even sneezing, has been implicated; these potentially rupture meningeal diverticula or cause tears in the dural nerve sheath⁸⁷.

Proposed diagnostic criteria for SIH include clinical and imaging findings that suggest intracranial hypotension, or directly demonstrate an active spinal CSF leak^{34,88-90}. According to the International Classification of Headache Disorders, third edition, SIH is diagnosed when headache has developed spontaneously and in temporal relation to a CSF leak (evident on imaging) and/or CSF hypotension (lumbar puncture opening pressure <60mmCSF⁸⁰). These criteria are probably the most widely accepted, but do not capture the full spectrum of patients with SIH. In fact, SIH is actually a misnomer, as the majority of patients exhibit opening CSF pressures within the normal range^{91,92}. The true pathophysiology is therefore more appropriately described as reduced intracranial

CSF volume rather than CSF hypotension^{93,94}. Moreover, low opening pressure is, however, an unreliable marker of the disorder because it has been reported in only a third of patients with confirmed spontaneous intracranial hypotension⁹⁵, and could have led clinicians to exclude this diagnosis in patients with normal pressure. This is why diagnostic criteria have changed significantly throughout the last few decades, and alternative diagnostic criteria have been proposed^{96,97}. These factors have probably contributed to the current uncertainty on how to reliably diagnose SIH and effectively treat these patients⁷⁹. For this reason SIH was misdiagnosed in up to 94% of individuals, most commonly as migraine, meningitis, psychological disorder, or even malingering¹⁰⁸.

The reasons why these patients with SIH have normal CSF opening pressure on LP might be related to the inadequate methods of measurement or to the actual absence of a low CSF pressure state. LP opening pressure is a snapshot method of measurement, it does not reflect the intracranial pressure in the upright position, and neither offer any information regarding the CSF dynamics during a postural change. The correlation between SIH and connective tissue disorders supports the hypothesis of a dural compliance disorder as the main cause for this syndrome^{98,99}. Although LP has a good sensitivity (67%) and can support the diagnosis of SIH, a normal opening pressure does not exclude this disorder; therefore, the diagnosis of SIH cannot be excluded in patients who do not present with all the typical features of this disorder⁷⁹.

The clinical manifestations of SIH are thought to result from increased efflux of CSF in the upright position, leading to traction on pain-sensitive fibres within the dura mater. Despite the variability and the great diversity of signs and symptoms orthostatic headache, particularly from occipital location, subsiding after lying down and worsening with Valsalva maneuvers, is the most common and hallmark symptom, affecting patients during their most active hours making SIH syndrome a debilitating chronic disease⁷⁹. Nonetheless, headache in SIH might be gradual or thunderclap in onset, less or more positional over time, even intermittent, and with no relationship with position, or become worse when lying down, and its intensity is variable⁹⁰. Also, the orthostatic headache, once believed to be an essential characteristic of SIH, is not invariably present and SIH should not be excluded based on the absence of orthostatic headache⁷⁹. Other signs and symptoms such as posterior neck or interscapular pain, horizontal diplopia caused by unilateral or bilateral cranial nerve VI palsy, nausea, emesis, radicular upper extremity symptoms, dizziness, blurred vision,

change in hearing, or obtundation may also be present⁷⁹ as a result of a decrease in CSF volume and sinking of the brain, but, as mentioned, patients with atypical clinical signs and normal CSF pressure may also be found^{85,100}. Cochlear vestibular manifestations (e.g., tinnitus, hearing change, and dizziness) are often seen¹⁰¹ and may be related to traction of the VIII cranial nerve, but an alternative and more plausible mechanism could be the alteration of pressure in the perilymphatic/endolymphatic inner ear fluid by alteration of the pressure gradient between CSF and perilymphatic fluid that are in contact at the level of the acoustic aqueduct. This would cause an endolymphatic hydrops such as Menière's syndrome¹⁰². Other atypical presentation of SIH, seen in older patients with SIH with a longer symptom duration, are memory deficits, dementia with frontotemporal features, parkinsonism, and ataxia¹⁰³. Tanaka et al found that more females and patients under 40 years of age reported "acute onset" and "severe" headache, whereas more males and patients over 40 presented with subdural hematomas and reported longer durations of symptoms before presentation¹⁰⁴. Whether these patterns reflect biologic features of SIH or reflect presentation bias trends is uncertain⁹¹. Due to the woefully inadequate awareness of it, the ratio of initial misdiagnosis and missed diagnosis is pretty high, and it also contributes to the long mean time (13 months) from symptom onset to diagnosis¹⁰⁵. Finally, in clinical grounds, despite not typically being considered a serious or life-threatening disorder, spontaneous SIH can cause considerable morbidity, result in substantial long-term disability, and (in rare cases) lead to decreased consciousness and coma^{93,106,107}. The mechanisms proposed in published work to account for this presentation include transtentorial herniation with compression of the diencephalon, and traction on cerebral sinuses resulting in deep venous thrombosis⁹³. As a result of low CSF volume—sagging of the brain—tension on the cranial nerves and the dura mater occurs, particularly in the posterior fossa, which is especially tension-sensitive¹⁰⁸.

A previous common misconception is that skull base CSF leaks cause intracranial hypotension; this is not generally the case⁹¹. Normally, when upright, gravity causes a gradient of increasing CSF pressure as one moves caudally along the spinal axis, with the result that intracranial pressure is slightly lower than atmospheric pressure in this position¹⁰⁹. This gradient disappears in the recumbent position. As a result of this physiology, spinal CSF leaks cause orthostatic headaches while leaks at the level of the skull base do not. Rather, skull base defects tend to leak CSF when patients

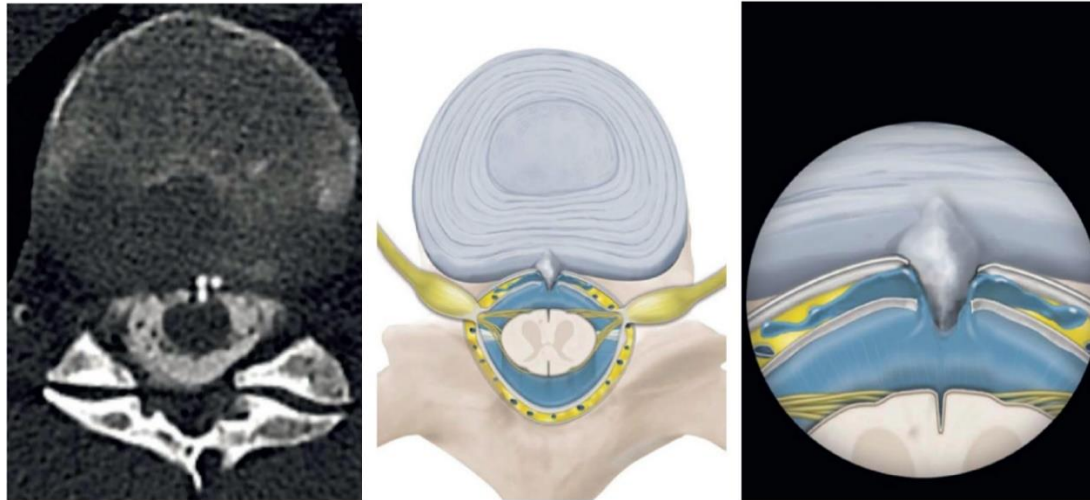
are bent over, leading to CSF rhinorrhea or otorrhea, not orthostatic headaches. This lack of association between SIH and skull base CSF leaks has been confirmed in a large series of patients with SIH¹¹⁰.

In non-syndromic patients with SIH, leaks are predominantly, if not exclusively, due to mechanical tears, CVFs, and leaking nerve root sleeves/meningeal diverticula and, according to that, they could be classified in four types¹¹¹.

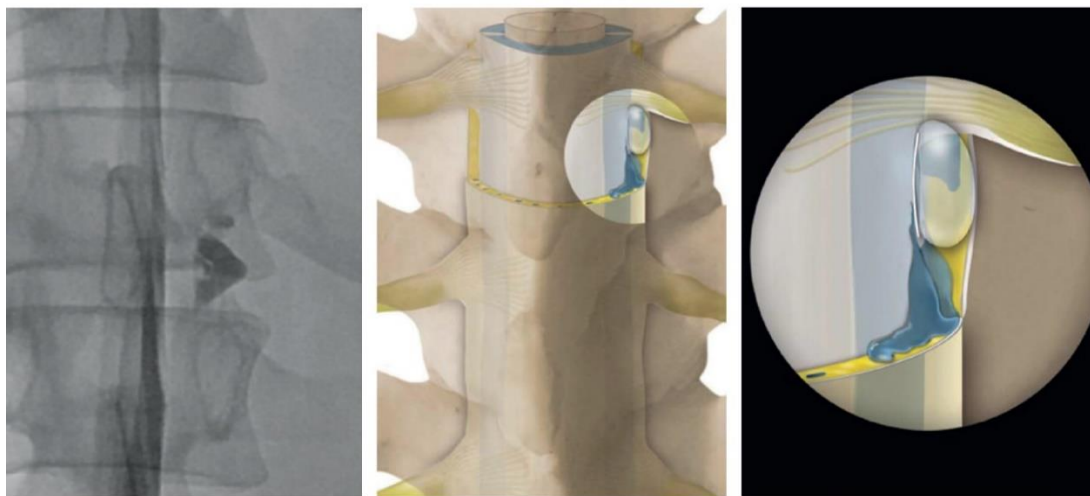
Type 1 leak, or dural tear type, is caused by degenerative disc disease caused by an osteo discogenic microspur (eg, a calcified disc protrusion, osteophyte or vertebral outgrowth) that pierce the dura like an ice pick, penetrating the thecal sac, and creating a mechanical tear in the ventral dura^{111,112}; nonetheless, conspicuous disc protrusions or large spinal nerve root cysts do not always correlate with the level of CSF leakage⁹³ (Fig 9). They are far more commonly located within the thoracic spine or lower cervical spine^{113,114}. The propensity for these locations may be due to the close apposition of the dura to the posterior aspect of the thoracic vertebral bodies and discs as a result of the normal thoracic curvature, combined with a higher rate of calcification of thoracic disc protrusions that can erode the dura to a greater degree than non-calcified disks^{91,115,116,117}. Patients with these ventral dural punctures are well-recognized as representing a large segment of patients with SIH, ranging from 26.6 to 48% of cases^{86,91}. All patients with type 1 show a typical ventral hole in the thecal sac on digital subtraction myelogram (DSM) or dynamic CT-myelography (DCTM)^{86,111,115} (fig. 10). Type 2 leak, or meningeal diverticulum type, is due to a more lateral tear in the dura due to leaking spinal nerve root diverticula/dural ectasia. These leaks are thought to arise from the base of the nerve root relating to a pre-existing thinned or dehiscence area of the dura in the axillary sleeve region of a nerve root. This herniated arachnoid may rupture, producing a fast CSF leak, or CSF may seep slowly from the margins of the dehiscence. Most commonly occur within the thoracic or upper lumbar spine and can have varied morphologies, in some cases solitary and in others complex and multilobulated¹¹⁷, (fig. 9). Its incidence ranges from 13 to 48% of cases^{86,112}. Nonetheless, diverticula are common, and one study found that the number and configurations of diverticula are similar between patients without and with CSF leak¹¹⁷. Therefore, patients with SIH may have leakage from a particular spinal meningeal diverticula among many others that turn out to be common incidental findings¹¹⁷ (Fig. 11). Also, periradicular leaks may not necessarily represent the precise site

of a CSF leak and lumbar puncture may cause an iatrogenic CSF leak¹¹⁸.

Fig. 9. Examples of the three types of CSF leak. Type 1: a ventrally located dural slit due to an osteo discogenic microspur (calcified disc protrusion or osteophyte) penetrating the thecal sac. CSF leaks into the epidural space. Type 2: a leaking spinal nerve root cyst. Type 3: a direct CSF-venous fistula. (Reproduced from Dobrocky T et al. Spontaneous intracranial hypotension: searching for the CSF leak. The Lancet Neurology 2002, with permission).
Type 1



Type 2



Type 3

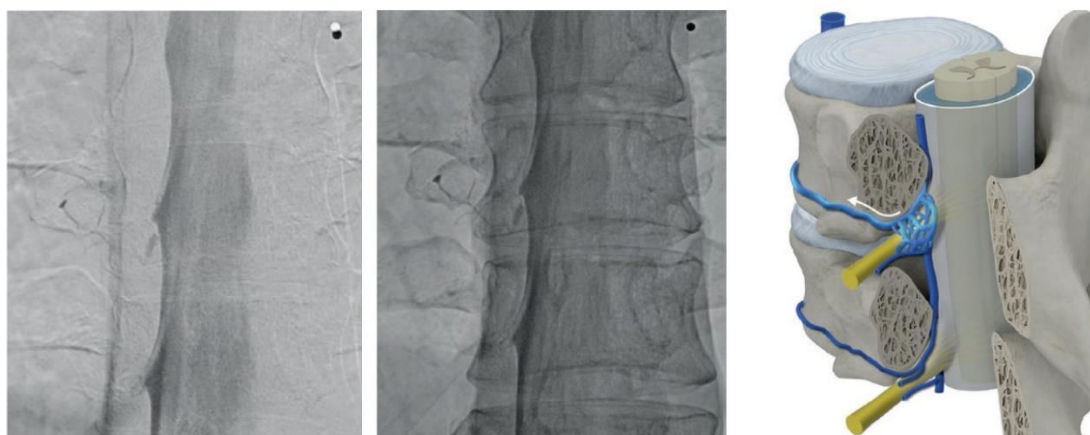
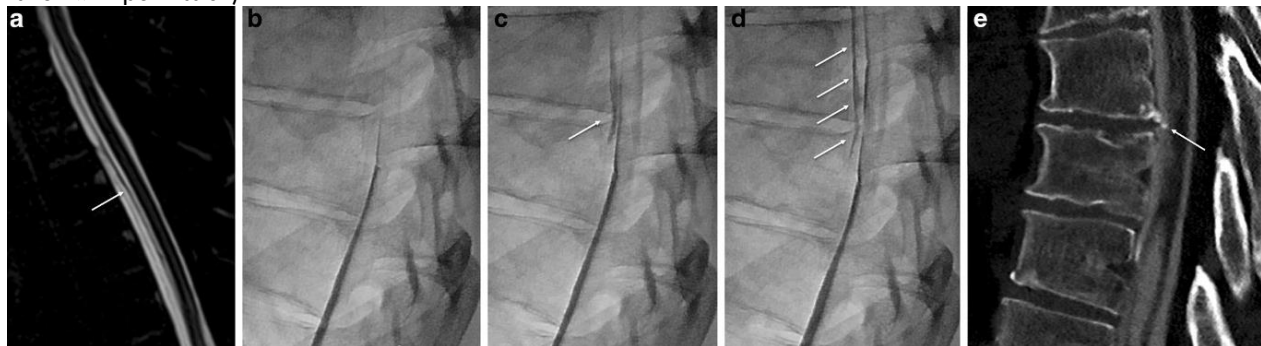


Fig. 10 (A-D). Middle-aged patient with sudden onset of orthostatic headache. A, heavily T2 weighted sagittal MRI with visible cerebrospinal fluid in the ventral epidural space, and the dura mater (arrow). B-D, dynamic myelography with contrast medium leaking into the ventral epidural space (arrow). E, postmyelography CT demonstrating a ventral microspur (arrow) at the corresponding level leading to a dural breach. (Reproduced from Piechowiak, El et al ¹⁵⁹, taken with permission).



Type 3 leak, or CVF, were discovered by Schievink et al¹¹⁹ and provided an extraordinary step forward in the care of patients with SIH, since it is a unique type of CSF leak because it is not associated with an extradural CSF collection^{110,121} (fig. 9). CVF are direct CSF-venous fistulas resulting from direct communications between the perineural subarachnoid space and surrounding veins. This aberrant connection allows unregulated loss of CSF back to the circulatory system^{120,121}. The reason for this, whether related to meningeal fragility or juxtaposition of CSF to the veins, remains speculative⁸². Most CVFs occur between T7 and T12 and are associated with a meningeal diverticulum in 82% cases¹¹² with the fistulous connection commonly originating from the diverticulum itself¹²¹. CSF-venous fistulas can also allow leakage into the epidural space in the absence of a dural tear¹²². Farb et al proposed¹¹² that an embryonic pseudomeningocele, masquerading as a diverticulum, first insinuates into the venous system and heals, aberrantly creating a 1-way CVF, which we categorize as type 3 CSF leak. This postulation also accounts for these CVFs being commonly but not invariably seen next to what appears to be a diverticulum. Its incidence is low, roughly 2,5%⁸⁶. Although its true incidence is not well established and probably higher than previously believed because tailored radiologic diagnosis is in progress¹²¹. Most commonly occur along thoracic nerve roots. Such fistulas should be considered as a potential etiology for SIH in patients where a CSF leak cannot be identified⁹¹. Surgical ligation of a CVF as described by Schievink et al^{110,123} or endovascular treatment¹²⁴ are the most efficacious treatment of these lesions.

Type 4 leak is the least common form of CSF leak and it results from a distal nerve root sleeve leak that does not fistulize into the venous system but

rather tracks into and dissipates into the adjacent facial planes¹¹².

Type 1 and 2 leaks typically lead to CSF effusion from the intrathecal space to the epidural compartment, resulting in a spinal longitudinal extradural CSF collection (SLEC)¹²⁵, and indicates a high-flow leak, typically type 1 or 2, and the need for an imaging method with good temporal resolution⁹³, whereas type 3 and 4 leaks typically do not result in SLEC⁸².

Fig. 11. Plain T2-weighted fat-suppressed spine MR images in a female patient with HIS and multiple meningeal diverticula. Coronal thoracic and upper lumbar spine reconstructed CISS images show multiple spinal diverticula.



IMAGING

On imaging grounds, although routine contrast-enhanced brain MRI protocols are sufficient to evaluate for intracranial features of SIH, specialized noncontrast spine MRI protocols designed to detect extradural CSF can obviate conventional invasive myelography and aid in planning further invasive tailored imaging tests for the workup of SIH^{11,126}. Once a leak or fistula is suspected on the basis of clinical features and/or non-invasive imaging, its location may be investigated by dynamic myelography, as a first step on mini-invasive procedures. If not, other most sophisticated mini-invasive procedures such as DCTM or CE-MRM should be performed.

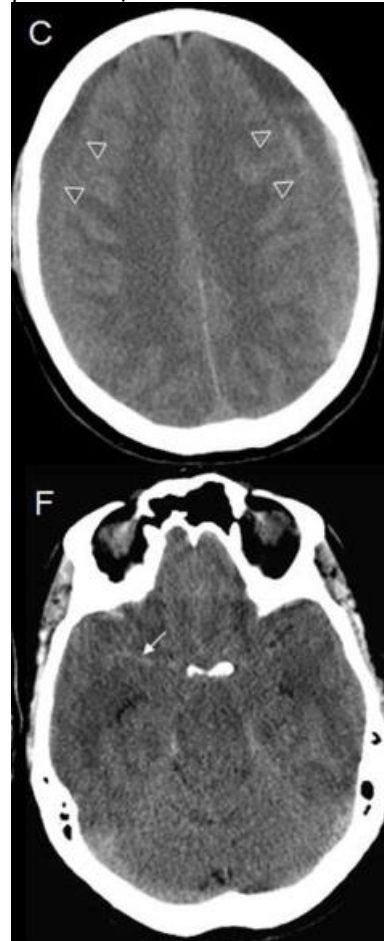
Brain

Many of the clinical and imaging manifestations of SIH can be explained by the Monroe-Kellie doctrine¹²⁷. This states that within a mature intact skull the sum of the intracranial volumes of brain, blood, and CSF is a constant. When CSF hypovolemia occurs one of the other two constituents must be compensated for by an increase in one or both of the others. As the volume of the brain cannot increase, blood volume increases, primarily within the more compliant venous circulation. Consequently, several abnormalities might be observed on brain imaging of patients with SIH. These abnormalities generally result from intracranial CSF loss and a compensatory increase in the blood compartment, resulting in hyperaemia⁹³.

Cranial CT

Although brain CT does not provide as many cardinal features as MRI, it is prior to more definitive imaging in the outpatients or emergency department and it is a helpful initial diagnostic tool for its non-invasive diagnosis⁹⁰. Brain CT is often unremarkable in the context of SIH and is generally less useful than cerebral MRI⁹⁰, but may show some of SIH neuroradiologic signs, such as engorged transverse venous sinuses, bilateral fluid collections (hygromas or subdural hematomas), small ventricles, obliteration of the prepontine cistern, brain swelling, and cerebral venous thrombosis, and increased attenuation in the basilar cisterns or along the tentorium cerebelli, which can mimic subarachnoid hemorrhage^{85,128,129} or “pseudo-subarachnoid haemorrhage” secondary to brain sagging, since a reduced CSF volume efface the basal cisterns and Sylvian fissures, causing prominence of relatively hyperattenuating arteries and veins¹³⁰ (fig 12).

Fig. 12 (A and F). Nonenhanced CT scan. A: Subdural hematomas (arrowheads) with minimal mass effect. F: Pseudo-subarachnoid haemorrhage. Notice increased attenuation in tentorium and cisterns/sylvian fissures (arrow). (Reproduced from Ferrante E et al¹²⁸ with permission).



Cranial MRI

In the initial evaluation of undifferentiated headaches, brain MRI is often performed without contrast, but in suspected cases of SIH, contrast administration is essential^{91,94,131}. On head contrast-enhanced MRI, diffuse regular pachymeningeal enhancement in both the supratentorial and infratentorial spaces is the most common imaging finding^{85,91,132} (fig. 13A), underlying the pathological substrate for this enhancement. Because the leptomeninges have a blood-barrier and pachymeninges do not, the latter are enhanced with Gd. This meningeal enhancement may be associated with additional imaging abnormalities including subdural fluid collections, occurring in about 50%⁸⁵. Dural thickening and hyperintensity can also be shown on FLAIR sequences but it can be difficult to distinguish from adjacent subdural fluid collections on this sequence so the use of contrast medium is considered essential^{132,133}. Several rare conditions can have a similar meningeal

appearance on MR imaging, such as idiopathic hypertrophic pachymeningitis, Immunoglobulin 4 (IgG4)-related disease¹³⁴, neurosarcoidosis¹³⁵, noninfectious and infectious granulomatosis¹³⁶⁻¹³⁸. Finally, post LP, postsurgical states, and neoplastic disorders, may show the same radiological pattern, although relevant history will distinguish these entities^{93,139}.

As stated, volume may also be replaced with subdural collections, either hygromas or hematoma, often bilaterally, and result from a decrease in the CSF volume within the fixed volume of the skull, leading to passive transudation of fluid out of the intravascular spaces in order to compensate for this volume loss. They are likely caused by tearing of bridging veins or bleeding from enlarged veins in the subdural zone^{89,91,127}. Bilateral hygromas or subdural hematomas secondary to SIH are important to exclude from other clinical settings and proper etiology must be identified because subdural fluid collections will not resolve until there is successful treatment of the underlying SIH (fig. 13 B-D). Moreover, if the collections are drained, they will recur due to the underlying abnormal CSF dynamics¹⁴⁰. Therapy should be focused on finding and treating the leak rather than drainage of the collections¹³⁹.

“Venous distension”, secondary to small thin-walled dilated blood vessels in the subdural space, is another specific indicator of decreased intracranial volume¹⁴¹. It is a feature of blood volume compensation as a consequence of CSF volume loss and is present in 75 to 93% of cases^{96,141}. It is reported that venous sinus thrombosis may be more prevalent in patients with SIH compared with general population for several reasons¹³⁹. Also, venous distension is the first sign to reverse after successful treatment of SIH⁸⁹.

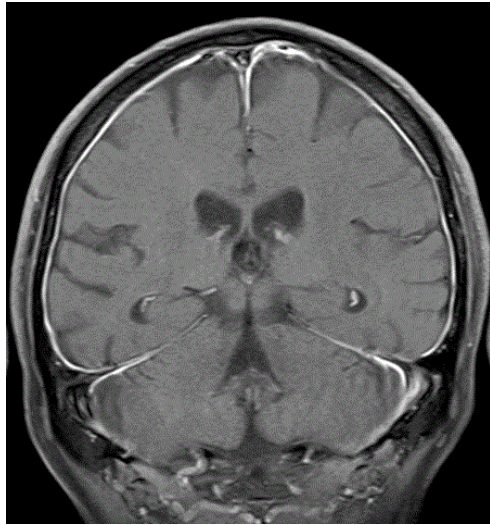
“Sagging” of the brain may be present when loss of buoyancy in the intracranial compartment occurs, as a result of the loss of volume of supporting CSF. It is an important imaging hallmark of SIH, encompassing several features such as ventricular collapse, bowing of the optic chiasm, flattening of the ventral pons against the clivus with obliteration of the prepontine or peri chiasmatic cisterns, drooping of the corpus callosum, ventricular system collapse, and cerebellar tonsillar descent^{85,139}. The prevalence of brain sagging in SIH is 51-62%^{88,121}.

Low-lying cerebellar tonsils or cerebellar tonsillar descent through the foramen magnum is usually seen in cases of very severe mid-brain sagging. However, it should be interpreted with caution when other findings of brain sagging are absent, since this sign is also present in Chiari malformation, a congenital condition that can be treated by posterior fossa decompression. Thus, it is especially important to distinguish this sign carefully, particularly as it can also be unreliable^{93,108}. Conversely, when cerebellar tonsillar ectopia is present in patients with headaches, the imaging should be scrutinized for other signs of brain sagging before the diagnosis of Chiari I is made¹⁰⁶. Moreover, individuals with Chiari malformation have other very important imaging features, are usually diagnosed at a much younger age, and present with different clinical symptoms compared with patients with spontaneous intracranial hypotension^{93,105}.

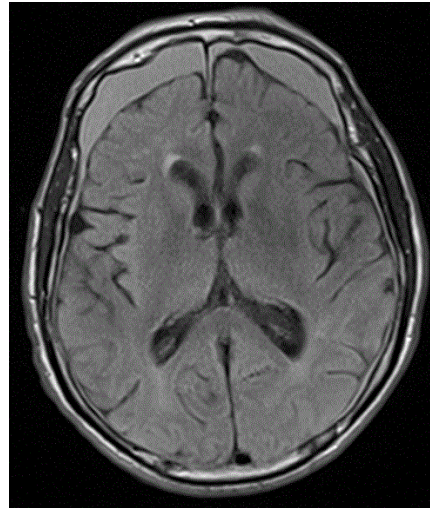
Typical findings of a leak are contained in the mnemonic SEEPS (subdural fluid collections, enhancement of the meninges, engorgement of venous structures, pituitary hyperemia, sagging of the brain) and are highly suggestive of the presence of a leak^{45,97}.

Superficial siderosis may occur as up as 50% of patients with chronic spinal CSF leaks and SIH¹⁴², as a result of repeated episodes of chronic subarachnoid haemorrhage from friable blood vessels at the margins of spinal dural defects and typically related to recurrent trauma from a spiculated osteophyte or disk protrusion¹⁴³ or because of tractions of the cerebellum and/or vermian veins on the skull base, leading to microhemorrhages and hemosiderin deposition¹⁴⁴, causing hemosiderin deposition on the surface of the spinal cord, brainstem and cerebellum. This appears as linear hypointensity, mainly on the infratentorial brain pial surfaces, on susceptibility-weighted imaging or T2*-weighted gradient echo imaging (fig. 13 E). Approximately 50% of patients with posterior fossa superficial siderosis have a spinal extradural CSF collection, indicating a CSF leak^{142,145,146}. Dural leaks causing recurrent subarachnoid bleedings can represent the single underlying cause for the superficial siderosis. The accumulation of this neurotoxic iron leads to progressive cell damage and neurological deficits¹⁴⁷.

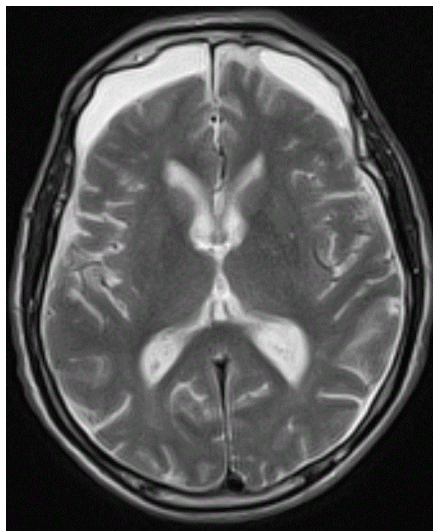
Fig. 13. Brain MRI features of HIS in a 56/y old female. A, coronal postcontrast T1-w image shows diffuse regular pachymeningeal enhancement in both the supratentorial and infratentorial spaces. B and C, axial FLAIR (B) and T2-W (C) images through the lateral ventricles showing bilateral subdural collections. D, axial post contrast T1-weighted image at the same level shows diffuse meningeal enhancement. E, axial susceptibility-weighted image (SWI) through the brainstem and cerebellum shows preferential hypointense signal throughout the subpial surface of cerebellar hemispheres and medulla oblongata consisting on chronic hemosiderotic deposits.



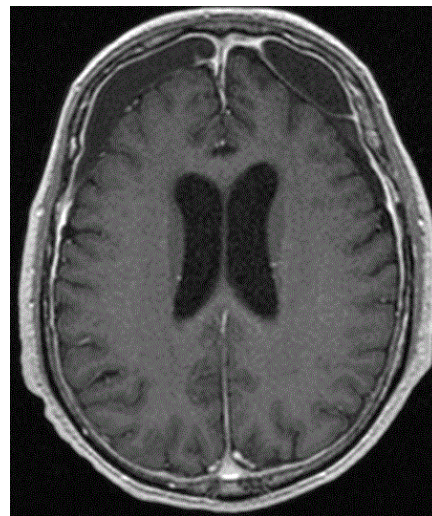
A



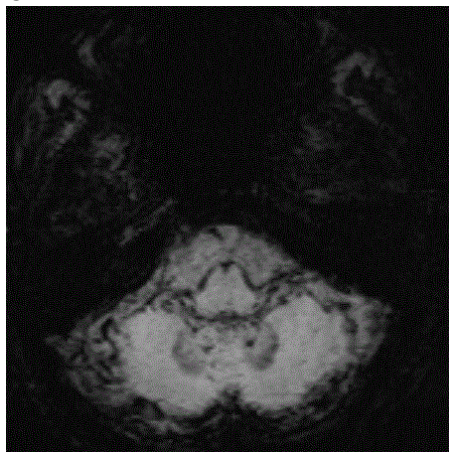
B



C



D



E

Engorgement of the pituitary gland (8–11 mm), secondary to venous congestion, causes enlargement of the gland with a convex superior margin, occurs in 38% patients with SIH¹³³, but is an unreliable sign of the condition, since gland size varies according to age and sex or an underlying infiltrative process, such as hypophysitis or adenoma, and care must be taken not to confuse this sign with physiologic enlargement as can be seen with pregnancy⁸⁵. Moreover, hyperprolactinemia can also occur in SIH and is associated with brain sagging, possibly indicating a stalk-effect as the mechanism¹³³.

Other MRI finding of SIH such as reduced optic nerve sheath diameter and diffuse calvarial hyperostosis are reported unreliable signs of SIH syndrome⁸⁹.

The number of brain imaging signs required for diagnosis of spontaneous intracranial hypotension has not been clearly defined, and reliable cutoff values for quantitative signs are absent, although smooth, generalised (i.e., evenly spread) dural enhancement is quite typical, no single imaging sign is specific for spontaneous intracranial hypotension. For the purpose of triaging patients suspected of SIH in whom brain MR imaging is suggestive and may benefit from more invasive or expensive myelographic examinations and subsequent targeted therapy, a radiological scoring system that integrates the 6 most reliable brain MRI findings has been proposed¹³¹. Pachymeningeal contrast enhancement, engorgement of the venous sinuses and effacement of the suprasellar cistern of 4.0 mm or less were shown to be the most important discriminating features between SIH patients and normal controls and weighted with 2 points each¹⁴². However, dural enhancement—the most common sign—was found to decrease in prevalence with time after symptom onset¹⁴⁸. This study suggests that the sensitivity of brain imaging may decrease in patients who have been leaking CSF for longer periods of time, perhaps as a result of compensatory physiologic changes. Consequently, it is possible that patients with chronic CSF leaks may exhibit different physiology, imaging, and treatment responses than those with acute leak¹⁰⁶. Finally, it has been estimated that up to 20% of patients with SIH have a normal brain MRI^{120,149}.

RADIONUCLIDE CISTERNOGRAPHY

RC, once used more extensively for spinal CSF leak localization, now is an elective initial indirect imaging test used in the evaluation of suspected SIH and, as it has had happened in the diagnosis of CSF-rhinorrhea and otorrhea, is rarely performed nowadays, and is increasingly

considered obsolete, because it does not show the precise localization of a leak and its inherent of poor spatial resolution and inferior anatomical delineations, its invasiveness, requiring LP, and radiation exposure^{97,105}. The literature pertaining to the use of this technique in patients with SIH is quite limited and RC, in general, is infrequently performed compared to anatomical imaging studies^{7,91,150,151}. Moreover, the greatest disadvantages of any mini-invasive procedure that require LP, apart from the complexity of the procedure, are iatrogenic CSF leaks¹⁵² and worsening symptoms¹⁵³ caused by lumbar puncture.

Nevertheless, RC can be used when initial brain and spine MR imaging are negative for signs of SIH in a patient with equivocal symptoms of SIH syndrome and may be helpful in this instance to determine whether to proceed to further invasive testing^{82,139}.

In a normal nuclear medicine cisternogram, there is complete coverage of the cerebral convexities 24 h after intrathecal tracer injection in the lumbar spine. Incomplete convexity coverage at 24 h suggests impairment of CSF flow dynamics, as can be seen in SIH. Other potential findings on cisternography which may suggest any CSF leak include early visualization of soft tissues and the bladder. If the cisternography is positive, the patient will typically undergo lateral decubitus DSM or CTM to assess for a possible SLEC leak⁸².

CSF PET with ⁶⁸Ga-DOTA, is a novel fast approach of RC for verification, though not localization, of spinal CSF leaks which hold promise for its high sensitivity and specificity, and it has the potential of the imaging methods to reduce the burden to the patient who eventually undergo other localizing invasive methods¹⁵⁴. Although further prospective studies are needed to be validated and it is also an expensive invasive method.

SPINE IMAGING

In the upright position, hydrostatic pressure in the spine is positive relative to atmospheric pressure, and pressure within the intracranial compartment is slightly negative with respect to atmospheric pressure¹⁰⁹. Therefore, the spine represents the anatomic source of most symptomatic CSF leaks and venous fistulas, such that investigation of the source of SIH should primarily focus on targeted imaging of the spine rather than the skull base, as mentioned earlier, because there is no causal association between SIH and cranial cerebrospinal fluid leaks^{110,126}. It is important to take in mind that not every patient with orthostatic headache should be subjected to multiple spine imaging tests particularly invasives, because they have the potential for adverse reactions (to

intrathecal contrast), may entail high radiation exposure, and are a financial burden on the healthcare system¹⁵⁶.

Identification and precise localisation of a CSF leak is the main goal. Although most leaks are reported in the thoracic spine and at the cervicothoracic junction, the leak can occur anywhere from the skull base to the sacrum. Therefore, when the spine is imaged the entirety of the spinal canal must be scrutinised for a dural breach that might be only the size of a pin⁹³. The main usefulness of a spinal MRI is to identify an area of in the epidural space, suggestive of the site of CSF leak^{85,139}. Whole spine MRI from the cranial-cervical junction to the sacrum with both T1 and T2 fat suppression sequences is a safe, non-invasive, and sensitive technique to identify spinal CSF leaks. They should be performed as a first-line clinical investigation whenever possible. Invasive imaging intrathecal-enhanced techniques that require LP should be reserved for patients without identified leak on spinal MRI, who have failed to respond to two or three epidural blood patches (EBPs) performed “blindly” and in whom a treatment targeted (EBP or surgery) at the site of a leak is being considered⁸⁵.

Plain and iv contrast enhanced T1-weighted spinal MRI

When SIH is suspected, plain and intravenous enhanced MRI of the entire spine is usually performed as a first-line clinical investigation. These procedures can support a diagnosis of SIH, but only rarely shows the location of the CSF leak. Moreover, plain spinal MRI may yield false-negative results because a collapse of the dural sac and epidural CSF accumulations are easily missed, yet is still an excellent method of demonstrating the extent of ventral spinal CSF leaks⁹⁰. Notice that as there are patients with SIH syndrome and no brain radiological features but positive of radiological spinal features, additional MRI of the brain head should be performed¹²⁴.

Spine imaging aims to classify and localise the site of CSF leakage as either i) a ventral dural leak; ii) a leaking spinal nerve root diverticulum, or iii) a direct CSF-venous fistula (fig. 9, 10, 14, 15, 16, and 17). Precisely locating the site of CSF leakage is fundamental to successful treatment, which includes a targeted EBP and surgical closure when conservative measures do not provide long-term relief⁹³. Plain and iv contrast enhanced T1-weighted fat suppressed spinal MRI may show abnormalities in 60-80% of patients^{102,124} and may demonstrate

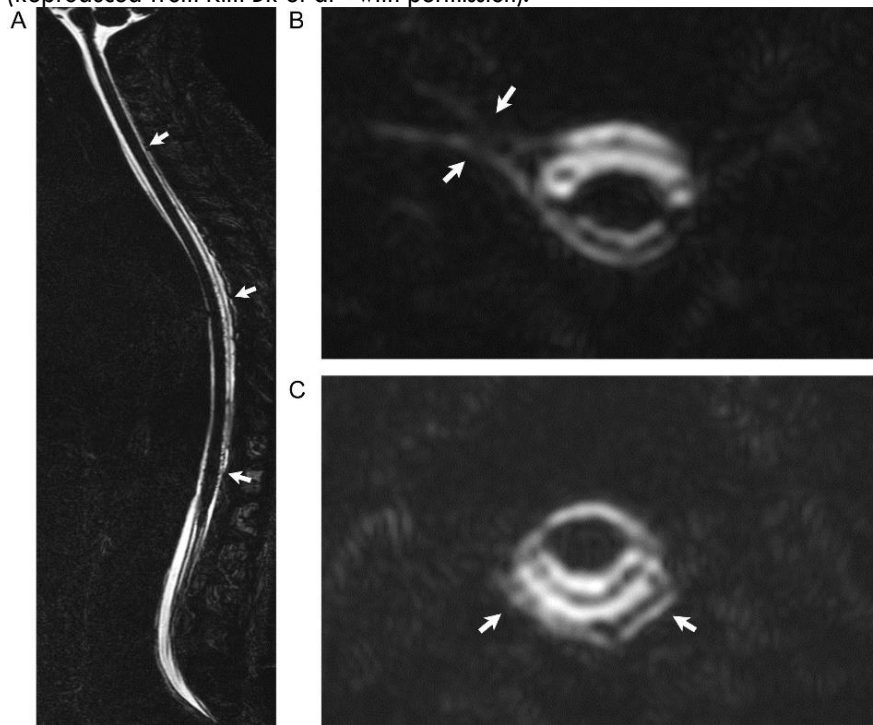
cervical pachymeningeal enhancement, non-compressive SLECs, fluid collection in soft tissues near the C1 and C2 vertebrae (it could be sometimes a CSF leak false localization sign), meningeal diverticula, dilated nerve root sleeves, engorgement of epidural venous plexus and SLECs, although it not always pinpoints the site of the leak. SLECs are mostly associated with nerve root sleeve leaks, may be of variable size, with some producing high-flow leaks, and others producing quite subtle leaks. CSF-venous fistulas are notable negative in this regard because they usually do not result in pooling of fluid in the epidural space, and therefore may be difficult to detect on plain spine MRI.

Non-contrast high-resolution T2-weighted MR myelography (NCHRT2W-MRM)

Before proceeding with any invasive spinal procedure the new gold standard sequence of spine MR imaging is the NCHRT2W-MRM of the whole spine (3D fast spin-echo HT2W) for detecting CSF leaks without lumbar puncture and radiation exposure. Previous studies¹² have shown that standard T2W-MRM was comparable to CE-CTC in diagnosing CSF leaks and is used to guide targeted EBP. Heavily T2-weighted MR myelography sequences are based on 3D isotropic steady-state free precession sequences (such as CISS or FIESTA)^{7,12,14,155}, which allow multiple plane reformats and are particularly helpful in demonstrating SLECs and in pinpointing the site of the dural breach (fig. 14). These sequences enhance CSF signals by suppressing the adjacent background signal. This new standard protocol overcomes the shortcomings of previous MRI protocols comprising 2D sequences that were sufficient to identify a dorsal or ventral epidural fluid collection, but CSF leaking laterally via a perineural cyst or lateral dural defect may not be readily detected on those previous spine MRI protocols. In addition, the 3D sequence allows for the reconstruction of image data using various techniques, including maximizing or minimizing CSF signal (MIP and MPR respectively tools). Therefore, NCHRT2W-MRM of the whole spine is warranted to evaluate not only the epidural space but also the paraspinal soft tissues for the presence of extradural CSF¹¹. Ancillary MR finding apart from epidural fluid collections includes distention of the spinal epidural veins, detected as prominent signal-intensity flow voids in the anterolateral epidural space with consequent collapsed dural sac, appearing as a hexagon-like contour in the axial plane, seen in 75%–100% of cases¹⁵⁶.

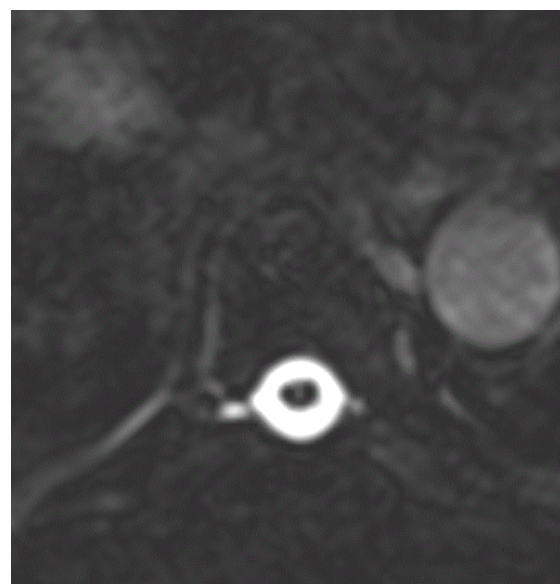
Fig. 14 (A-C). Central canal-type CSF leak. Whole spine sagittal 3D heavily T2-weighted MR myelography demonstrated diffuse CSF leak, from cervical to lumbar level (A) in a 45-year-old female patient.

Axial image of heavily T2-weighted MR myelography revealed CSF leak at the epidural space in the central canal and the right neural foramen, at C7/T1 level (B) and revealed posterior epidural CSF leak at the T4/5 level (C). (Reproduced from Kim BR et al¹³ with permission).



The presence, complexity, and laterality of meningeal diverticula can inform patient positioning for further lateral decubitus dynamic myelography. Careful scrutinization and comparison between the contours of meningeal diverticula often leads to detect elusive leaks coming from meningeal diverticula. Advantages of this first step non-invasive test are acknowledged, because it lacks invasiveness and it is easy to perform, resolving many cases. Shortcoming includes that fluid seen in retrospinal soft tissues might not correspond to the leak site and is a false localising sign¹⁵⁷. Also, fluid-filled structures (paravertebral veins and the cystic dilatation of nerve root sleeves or meningeal diverticula or unsuppressed fat, both of which exhibit hyperintensity on NCHRT2W-MRM similar to that of CSF), may be misinterpreted as CSF leaks because the suppression of background signals may cause poor anatomical orientation¹⁵⁷ (fig. 15).

Fig. 15. NCHRT2W-MRM axial reconstructed CISS fat-suppressed image of the spine shows fluid-filled structures (paravertebral veins and the cystic dilatation of nerve root sleeves or meningeal diverticula) both of which exhibit hyperintensity on MR myelography similar to that of CSF, that could be misinterpreted as CSF leaks because the suppression of background signals may cause poor anatomical orientation.



The presence, complexity, and laterality of meningeal diverticula can inform patient positioning

for further lateral decubitus dynamic myelography. Careful scrutinization and comparison between the

contours of meningeal diverticula often leads to detect elusive leaks coming from meningeal diverticula. Advantages of this first step non-invasive test are acknowledged, because it lacks invasiveness and it is easy to perform, resolving many cases. Shortcoming includes that fluid seen in retrosinal soft tissues might not correspond to the leak site and is a false localising sign¹⁵⁷. Also, fluid-filled structures (paravertebral veins and the cystic dilatation of nerve root sleeves or meningeal diverticula or unsuppressed fat, both of which exhibit hyperintensity on NCHRT2W-MRM similar to that of CSF), may be misinterpreted as CSF leaks because the suppression of background signals may cause poor anatomical orientation¹⁵⁷ (fig. 15).

These non-invasive methods are excellent in enabling identification of epidural CSF collection, but lack temporal resolution¹⁵⁸, thus hampering identification of CVF leak type¹⁵⁹. Moreover, the presence of SIH on brain imaging with no visible epidural fluid collection on spine imaging may therefore indirectly suggest that the source of CSF loss is attributable to a CVF. Direct identification of a CVF, however, relies on identification of shunting from the CSF to the venous system rather than on static anatomic abnormalities such as pooled epidural fluid. As a result, conventional spine MRI cannot directly detect CVFs^{121,159}.

Determining the presence or absence of SLECs dictates technique and positioning for advanced mini-invasive myelography techniques. The subsequent work-up varies by institution, reflecting local expertise and philosophy. Nerve root sleeve diverticula are commonly seen, though these are nonspecific and of unclear significance unless they are very large and irregular^{85,160}.

Fluoroscopy-based procedures and cross-sectional CT myelography

Myelographic techniques are broadly classified into fluoroscopy-based methods, including digital subtraction myelography (DSM), dynamic fluoroscopic myelography (DFM), and cross-sectional methods, such as decubitus contrast-enhanced CT myelography (CE-CTM) and dynamic contrast-enhanced CT myelography (DCTM). The techniques differs in the use of different X-ray technologies, whether conventional, digital subtraction acquisitions rooms (fluoroscopy-based methods), or advanced CT multi detectors scanners facilities, and that in the position the patients are positioned based on the type of suspected leak. Also, these techniques varies in terms of temporal resolution being the highest DFM procedure¹⁵⁹. The DFM has the highest temporal resolution but has a limited area of coverage inherent to the size of the flat panel detector, a limitation that DSM has not,

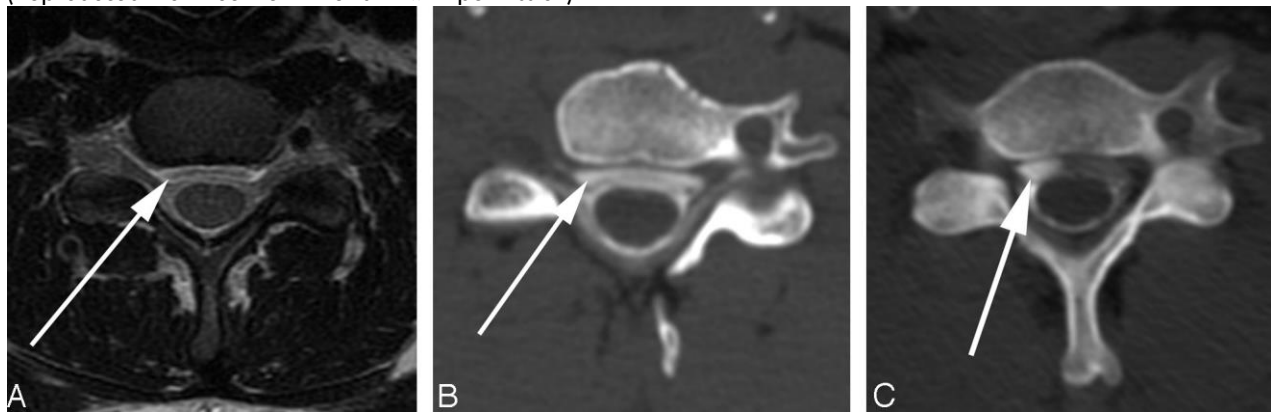
but both are extremely susceptible to breathing and motion artifacts. Both have an unfavorable dosimetry due to the use of multiple acquisitions, but DSM delivered approximately 2-4 fold more radiation than DFM during a 5s exposure¹⁶¹.

Radiation exposure in all these procedures is significant and has been reported with 19.7 (3.2–82.4) mSv for DCTM compared to 6.6 (1.2–17.7) mSv per DSM study¹⁴⁴. A limitation inherent to both DSM and DFM is the use of planar rather than computerized cross-sectional imaging. Also, an additional drawback of DFM is the lack of subtraction of background tissues, which can make detection of subtle CVFs more difficult^{107,159}.

DFM technique does not require general anesthesia because no subtraction mask is used while DSM does, and it has the unique capability of visualizing contrast dye within seconds of intrathecal injection and its escape into the epidural space through the dural tear (fig. 10). The principal drawback of DFM is the lack of subtraction of background tissues, which can make detection of subtle CVFs more difficult and it is also more operator dependent than other techniques. For this reason, most referral centers use DSM rather than DFM, and it is likely that DSM is more sensitive as a screening technique if no particular site of CVF is already suspected¹⁰⁷.

DCTM is a very valuable cross-sectional technique. It combines both high temporal and spatial resolution, and is used particularly useful at the cervicothoracic junction where superimposed bony structures of the shoulder and rib cage can obscure the leakage point on planar imaging¹¹¹, (fig. 16); however, owing to the time delay between scans it does not match the temporal resolution of real-time DSM where multiple frames are acquired per second. Furthermore, DCTM is associated with a higher radiation dose and should therefore cover only the few vertebral levels suspected of harboring the leakage site. In clinical practice, DCTM is cautiously used in patients in whom previous methods have failed to identify the leakage point¹⁵⁹. Non-dynamic CE-CTM techniques are best to localize suspected slow leaks, particularly using the new latest refinement upgrade (Dual Energy CT Myelogram) which increases the conspicuity of subtle CVFs compared to background and also helps in differentiating between calcified osteophytes and extradural contrast leaks¹⁶², while dynamic techniques, are best suited for localizing suspected fast leaks, for its capability of visualizing contrast dye within seconds of intrathecal injection and its escape into the epidural space through the dural tear, which would otherwise spread over many levels, obscuring the actual leakage site^{90,92,163}.

Fig. 16 (A-C). Fast CSF leak with spinal extra-arachnoid fluid collection requiring dynamic DCTM for leak localization. A, a fluid collection ventral to the thecal sac is seen on axial T2-weighted fat-suppressed image. B, non-dynamic CE-CTM (B) shows a ventral contrast collection from C3 through T9, but the site of leak cannot be specified. C, DCTM shows extra-arachnoid contrast accumulating ventral to thecal sac at C6-C7, consistent with a ventral leak at this level. (Reproduced from Luetmer PH et al⁹² with permission).



The work-up varies among institutions, reflecting local expertise and philosophy, having in mind that the performance of these techniques may require sedation or general anesthesia⁸². A general principle is to position the patient prone for suspected ventral dural tears and lateral decubitus for a CVF or leaking diverticulum, to encourage gravitational contrast medium flow through the site of leakage. The laterality of a CVF cannot be predicted so both sides must be examined in case the first study is negative or, as occurs rarely, there are bilateral CVFs¹⁶³. A dynamic DCTM has the advantages of full spine imaging if needed and direct visualization of the leak location and offending osteophyte. However, this requires meticulous technique and custom-built cushions, is uncomfortable for some patients, has limited temporal resolution, and uses several CT passes requiring relatively high radiation dose. DSM largely lacks these advantages (and disadvantages) of DCTM but has higher temporal resolution. If a leak is not identified on dynamic prone DCTM (or DSM), a lateral decubitus DCTM or DSM is performed to evaluate for a lateral leak, although some lateral leaks will be identified on the initial prone imaging⁸².

In all these procedures iodinated contrast media is injected into the intrathecal compartment by LP (intrathecal 10-16 mL of 300 mg/mL iodinated contrast⁸²). The contrast is distributed by the patient elevating their pelvis before scanning. The study is then acquired as soon as possible during a breath-hold in maximum inspiration, to reduce motion artefact and increase the conspicuity of CVFs¹⁶⁴. Images are reconstructed with thin sections and a small field of view to maximise spatial resolution. An additional reconstruction including the kidneys is recommended as patients

with spinal CSF leaks can show early renal excretion of myelographic contrast medium, through absorption of leaked contrast medium by epidural veins or by direct passage into the venous system via a CVF¹⁶⁵. In cases of dural tears and leaking diverticula, DCTM shows extradural contrast medium. Contrast medium may diffuse rapidly from the leak site into an extradural CSF collection, obscuring the point of communication.

When there is a CVF, DSM, post myelography CTM, and DCTM may show the hyperdense paraspinal vein sign, due to a increased attenuation of the paraspinal veins after intrathecal administration of iodinated contrast material, indicative of the presence of a CVF and opacification of small foraminal radicular veins adjacent to a meningeal diverticulum or opacification of the epidural venous plexus¹⁶⁶. For some authors DCTM is the main imaging method used for diagnosis of CSF-venous fistulas^{93,105}. Nevertheless, lateral decubitus positioning during DSM or CE-CTM has been reported to provide a five-fold increase (from 15% to 75%) in detection rate of CSF-venous fistulas¹⁶⁷. Similarly the lateral decubitus position might increase the visibility of CSF-venous fistulas on imaging¹⁶⁸ and it is believed to be due to amplified concentration of contrast in the most inferior portion of the thecal sac, including the spinal nerve root cysts at which the fistulous connection is usually located¹⁶⁹. In all cases an early phase DCTM imaging is performed immediately after administration of intrathecal contrast material to detect rapid egress of CSF through a meningeal defect or CVF. In addition, a leak or fistula may be elicited by provocative maneuvers including pressure augmentation, patient elevation, and inspiration^{164,170}. A post myelography CT restricted to the level of leakage should be done immediately

after the early phase to identify underlying osseous pathology, such as bony spurs of the vertebral endplates or calcified disc protrusions.

On post myelography DCTM, a CSF-venous fistula might be recognised as a tubular opacified structure (i.e., hyperdense paraspinal vein sign) extending from a nerve root sleeve cyst or the thecal sac into the paravertebral space^{105,122,171,172}. Also, post myelography CT can also provide indirect evidence of CSF leakage. Some studies have shown renal pelvic opacification on post myelography CT in patients with a CSF leak or CSF-venous fistulas compared with patients without spontaneous intracranial hypotension^{173,174}. This finding probably indicates increased spinal CSF resorption from the epidural space in patients with SLEC and direct flow of intrathecal contrast (and CSF) to the bloodstream via CSF-venous fistulas in patients without SLEC⁹³.

DCTM may show several abnormalities:

1. Extra-arachnoid fluid that is focal or extending across several vertebral levels (in extreme cases, from cervical all the way to the lumbar level), (fig 16).
2. Meningeal diverticula (single or multiple, various sizes, different levels) may or may not be the site of CSF leakage even when large.
3. Extradural egress of contrast extending into the paraspinal soft tissues.
4. Direct CVF^{167,172}.

In short, DCTM is the most reliable test to show the exact site of leak. It also provides an opportunity to measure the CSF opening pressure. The rate of CSF leak may range from very slow to very fast⁸⁵. Hyperdense paraspinal vein sign could be also seen as a marker of CVF in both CE-CTM or DCTM¹⁷².

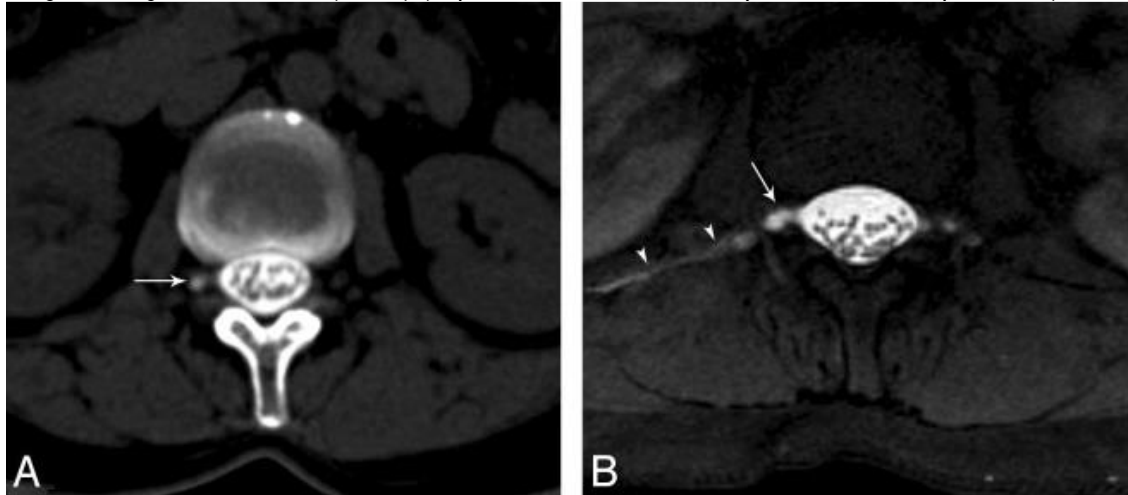
Contrast-enhanced MR Myelography (CE-MRM)

CE-MRM typically creates images based on fat-suppressed T1-weighted (T1W) images with a diluted paramagnetic contrast agent^{6,175}. The

advantages of the technique include high contrast resolution and no risk of radiation exposure but not fairly high spatial and time resolution. Although off label, is considered a safe and effective method for detection of CSF leaks¹⁷⁶. However, infrequently it has been associated with major adverse outcomes⁴⁶. Therefore, it should be reserved for problem solving in specific patients when other diagnostic techniques are not available or have failed and a high suspicion of leaks^{82,93}, particularly if SLECs have been identified in other non-invasive imaging techniques (i.e., plain MR or NCHRT2W-MRM) and so the suspicion of CVF is low.

Previous studies regarding the efficacy of CE-MRM for demonstrating CSF leaks reported higher sensitivity with CE-MRM than CE-CTM¹⁷⁷⁻¹⁷⁹ (fig 17), with the advantage of no radiation exposure. For these reasons some centers perform CE-MRM as first line imaging approach from the minimally-invasive radiological techniques. In particular, the literature suggests that slow leaks, which may not be evident on early phase imaging on DCTM, may be optimally detected with CE-MRM^{125,177,176,180}. This difference may reflect a combination of improved tissue contrast resolution for MRI compared with CT as well as the substantial delay in imaging for CE-MRM¹²⁶. When pressure-augmented decubitus dynamic CE-MRM is performed the pressure augmentation is anticipated to increase the conspicuity of extrathecal contrast material originating through slow or subtle leaks¹⁸¹. Using these combinations of techniques, several leaks that were occult on DCTM or NCHRT2W-MRM imaging could be detected. Latest imaging improvements suggest that CE-MRM using T1-weighted gradient echo high-resolution isotropic volume excitation MR (THRIVE) is optimal for this purpose increasing the diagnosis yield, detecting leakage of CSF from subarachnoid space to epidural and/or paravertebral space. In one study this specific technique showed 90% sensitivity of for detecting CSF leaks in patients with SIH³⁴.

Fig. 17 (A and B). A, axial CE-CTM image shows a right meningeal diverticulum (arrow) without CSF leak at the level of L1. B, axial T1-weighted fat-saturated CE-MRM image reveals both a CSF leak on the right side (arrowheads) and a right meningeal diverticulum (arrow). (Reproduced Taken from Albayram S et al⁶ with permission).



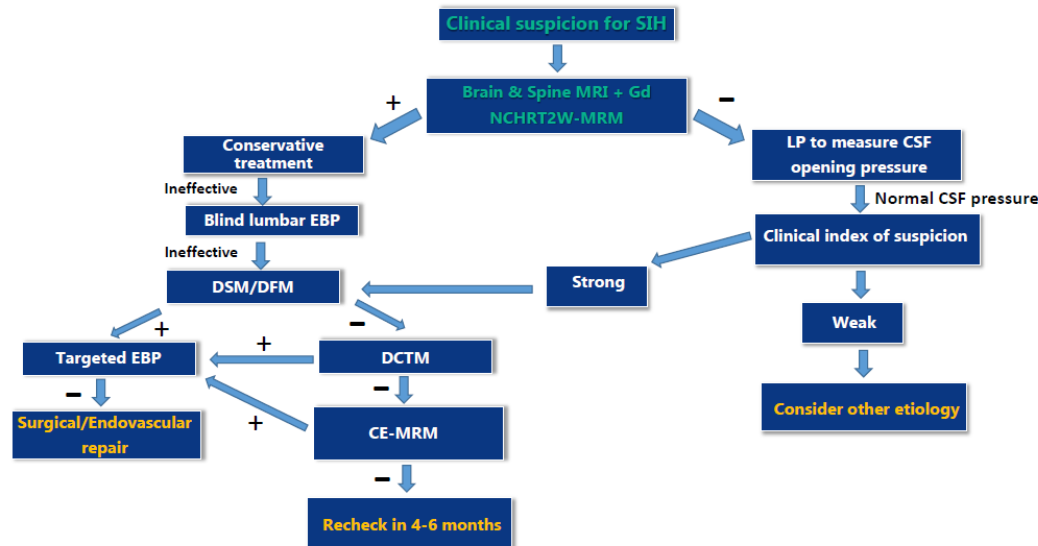
In order to diagnose the few CVF that could be missed in both conventional or CE-CTM and CE-MRM techniques some authors have proposed to perform both sequences consecutively, since the first one has the highest spatial resolution and the second the highest contrast resolution. However, only a few minutes of delay between intrathecal contrast application and imaging may obscure the leakage point, since contrast may span several vertebral levels, making localization impossible¹⁵⁹. This double test requires prior intrathecal injection of both paramagnetic and iodized contrast material.

Critical Comparison of Spinal Imaging Techniques for CVF Detection

Optimal techniques for detection of CVFs are still being developed. Comparison of imaging modalities for detecting CVFs has so far been limited to retrospective reports of CVFs confirmed using one imaging technique but not seen on previous imaging; such investigations are subject to selection bias that favors the modality used as the reference standard. Utilization of different imaging techniques is currently largely driven by the availability of imaging equipment and operator preference¹⁶⁶. Considering the broad, and growing,

clinical spectrum of spontaneous CSF leaks and substantial variability in many of its various aspects, a “what to do” algorithm is both important and complex, and will likely become even more complex in the future⁸⁵. According to the proposed diagnostic algorithm in Table 2 (from Ferrante et al⁸⁵ with modifications), patients with findings of SIH on brain MRI and or spine will follow, at first, conservative treatment. If ineffective, patients will undergo one or two blind lumbar EBP. If again ineffective, mini-invasive imaging studies will be required as proposed, starting from decubitus CE-CTM to evaluate for CVF if no extradural collection have been found on spine imaging. If decubitus CE-CTM is normal, then the patient returns on a separate day to undergo DCTM in the opposite decubitus position. During the second myelogram, 0.2 mL of intrathecal GBCA is simultaneously instilled for subsequent CE-MRM, which is performed within 30–60 minutes after dynamic CTM. After sagittal whole-spine acquisition, real-time monitoring is performed to prescribe additional axial and coronal planes of interest, with the goal of minimizing scan time while optimizing image quality¹²⁶.

Table 2: Diagnostic algorithm for skull base CSF leaks (Taken from Ferrante et al⁸⁵ with modifications). Gd: Gadolinium; CE-MRM: contrast-enhanced MR-myelography; DCTM: Dynamic CT-myelography; DSM: Digital Subtraction Myelography; DFM: Dynamic fluoroscopic myelography; EBP: Epidural Blood Patches; LP: Lumbar Puncture; NCHRT2W-MRM: Non-contrast High-Resolution T2-weighted MR-myelography.



Treatment

Treatment of SIH is beyond the scope of the paper. Readers are directed to comprehensive reviews of this topic^{79,82,90,91,107,156,155,176}.

To date, treatment recommendations have been based on expert recommendations or anecdotal experience. The limited data that exists in the literature on treatment outcomes are predominantly derived from retrospective, uncontrolled case series. Many of the available outcomes studies lack structured or validated outcomes measures, and no prospective outcomes studies or randomized investigations comparing various treatments have been published so far^{82,91}. Management of SIH relies on observational data and expert opinion^{85,91}. Still, some commentaries are necessary.

Treatment for spinal CSF leaks can be divided into conservative therapy, epidural patching, open surgery, or endovascular procedures. Because in some cases SIH resolved spontaneously or with only conservative treatment many patients did not undergo advanced imaging techniques at first⁸⁵. Conservative approaches include strict bed rest, appropriate liquid, caffeine and theophylline, analgesic, non-steroidal drugs and abdominal binders^{90,176,182,183}. Usage of steroids remains controversial.

If orthostatic headache persists after conservative treatment, an EBP without previous leak identification (so-called “blind” EBP) is widely used as initial intervention and may be repeated

several times. If EBPs fail, CSF leak sites identification performing mini-invasive imaging techniques is warranted.

Once the the site of fistula is identified a targeted EBP, surgical reduction of dural sac volume, or direct surgical closure^{85,159} is usually performed. However, when CSF source is diagnosed surgical or endovascular approach is the treatment of choice. The prognosis is generally good after intervention, but serious complications may occur. Unfortunately, the source of the leak may remain occult despite advanced imaging in an estimated 46%–55% of patients^{139,172}.

Corollary

SIH is an underdiagnosed cause of headache that results from spinal leakage of CSF. MRI of the brain shows one or more characteristic features in many patients but can be normal in a significant minority, further delaying the diagnosis. Patients may respond to conservative treatment or non-targeted EBP, but in refractory cases myelography is needed to locate the leak. A range of myelographic techniques are available, the choice will depend on both the suspected cause of the leak, the available resources, and preferences of the operator. Once the leak site has been located, the patient can be offered site-targeted patching with blood or fibrin sealant, neurosurgical, or endovascular repair. Neuroradiologists play a critical role in the management of these patients from the initial diagnosis, to precise localisation of

leak site and then minimally invasive targeted treatment or endovascular treatment in cases of CVF.

Prior publication

The submission has not been previously published, nor it has been sent to another journal for publishing.

Authors' contributions

AM initiated and designed the study. AM, and AO were involved in the interpretation of results and drawing conclusions. AM wrote the first draft of the manuscript. Both authors have read and approved the final manuscript.

Availability of data and materials

The datasets used and/or analyzed during the current study are available from the corresponding author on reasonable request.

Funding

Not applicable.

Declarations**Ethics approval and consent to participate**

This study did not require official or institutional ethical approval.

Consent for publication

Not applicable.

Competing interests

The authors declare that they have no competing interests.

REFERENCES

1. Chiapparini L, Farina L, D'Incerti L, Erbetta A, et al. Spinal radiological findings in nine patients with spontaneous intracranial hypotension. *Neuroradiology*. 2002;44:143-52.
2. Ferrante E, Savino A, Sances G, & Nappi G. Spontaneous intracranial hypotension syndrome: report of twelve cases. *Headache*. 2004; 44:615-622.
3. Moriyama E, Ogawa T, Nishida A, Ishikawa , & Beck H. Quantitative analysis of radioisotope cisternography in the diagnosis of intracranial hypotension. *J Neurosurg*. 2004;101:421-426.
4. Spelle L, Boulin A, Tainturier C, Visot A, Graveleau P, & Pierot L. Neuroimaging features of spontaneous intracranial hypotension. *Neuroradiology*. 2001;43:622-627.
5. FE: Watanabe Y, Makidono A, Nakamura M, & Saida Y. 3D MR cisternography to identify distal dural rings: comparison of 3D-CISS and 3D SPACE sequences. *Magn Reson Med Sci*. 2011;10:29-32.
6. Albayram, F. Kilic, H. Ozer, S. Baghaki, N. Kocer, C. Islak Gadolinium-enhanced MR cisternography to evaluate dural leaks in intracranial hypotension syndrome *Am J Neuroradiol*. 2008;29:116-121.
7. Yoo HM, Kim SJ, Choi CG, Lee D, et al. Detection of CSF leak in spinal CSF leak syndrome using MR myelography: correlation with radioisotope cisternography. *Am J Neuroradiol*. 2008;29:649-654
8. Speck U. Magnetic resonance ventriculography with gadolinium DTPA: report of two cases. *Neuroradiology*. 1997 39:418-422.
9. Algin O, Hakyemez B, Gokalp G, Ozcan T, et al. The contribution of 3D-CISS and contrast-enhanced MR cisternography in detecting cerebrospinal fluid leak in patients with rhinorrhoea. *Br J Radiol*. 2010;83:225-32.
10. Selcuk H, Albayram S, Ozer H, Ulus S, et al. Intrathecal gadolinium-enhanced MR cisternography in the evaluation of CSF leakage. *Am J Neuroradiol*. 2010;31:71-75.
11. Tay ASS, Maya M, Moser FG, Nuño M, Schievink WI. Computed tomography vs heavily T2-weighted magnetic resonance myelography for the initial evaluation of patients with spontaneous intracranial hypotension. *JAMA Neurol*. 2021;78:1275-1276.
12. Wang YF., Lirng JF, Fuh, JL, Hseu SS, & Wang SJ. Wang Heavily T2-weighted MR myelography vs CT myelography in spontaneous intracranial hypotension. *Neurology*. 2009;73:1892-1898.
13. Kim BR, Lee JW, Lee E, Kang Y. Utility of heavily T2-weighted MR myelography as the first step in CSF leak detection and the planning of epidural blood patches. *J Clin Neurosc*. 2020;77:110-115.
14. Tsai PH, Fuh JL, J.F. JF, Wang SJ. Heavily T2-weighted MR myelography in patients with spontaneous intracranial hypotension: a case-control study. *Cephalalgia*. 2007;27:929-934.
15. Algin O, Hakyemez B, Parlak M. Phase-contrast MRI and 3D-CISS versus contrast-enhanced MR cisternography on the evaluation of the aqueductal stenosis. *Neuroradiology*. 2010;52:99-108.
16. Algin O, Hakyemez B, Parlak M. Phase-contrast MRI and 3D-CISS versus contrast-enhanced MR cisternography for the detection of spontaneous third ventriculostomy. *J Neuroradiol*. 2011;38:98-104.
17. Brash RC. Methods of contrast enhancement for NMR imaging and potentials applications. *Radiology*. 1983;147:781-788.
18. Hinshaw DB, Wong VC. Paramagnetic contrast agents in the evaluation of brain neoplasms. *Top Magn Reson Imag*. 1989;1:79-93.
19. Sanjay S. Advances in contrast-enhanced MR: Principles. *Am J Roentgenol*. 1991;156:236-239.
20. Muñoz A. Magnetismo y susceptibilidad magnética. Diamagnetismo y paramagnetismo. Ferromagnetismo y superparamagnetismo. El efecto paramagnético de la melanina. Mecanismos de acción de los agentes de contraste en RM. *Radiología*. 1992;34:379-384.
21. Muñoz A & Castillo M. Indications for adult and pediatric magnetic resonance imaging gadolinium-enhanced cisternography and myelography: Experience and review of the literature. *Current Med Imag Review*. 2008;4:170-180.
22. Zeng QY, Xiong L, Jinkins JR, Fan Z, Liu Z. Intrathecal gadolinium-enhanced MR myelography and cisternography: a pilot study in human patients. *Am J Roentgenol*. 1999;173:1109-1115.
23. Jinkins JR, Rudwan M, Krumina G, Turgut TE. Intrathecal gadolinium-enhanced MR cisternography in the evaluation of clinically suspected cerebrospinal fluid rhinorrhea in humans: early experience. *Radiology*. 2002; 222:555-559.
24. Aydin K, Guven, Sencer S, Jinkins JR, et al. MRI cisternography with gadolinium-containing contrast medium: its role, advantages and limitations in the investigation of rhinorrhea. *Neuroradiology*. 2004;46:75-80.
25. Aydin K, Terzibasoglu E, Sencer S, Sencer A, et al. Localization of cerebrospinal fluid leaks by gadolinium-enhanced magnetic resonance cisternography: a 5-year single-center experience. *Neurosurgery*. 2008;62:584-891.
26. Di Chiro G, Knop RH, Girton ME, Dwyer AJ, et al. MR cisternography and myelography with Gd-DTPA in monkeys. *Radiology*. 1985;157: 373-77.

27. Jinkins JR, Rudwan M, Krumina G, Turgut TE. Intrathecal gadolinium-enhanced MR cisternography in the evaluation of clinically suspected cerebrospinal fluid rhinorrhea in humans: early experience. *Radiology* 2002;222:555–559.
28. Tali ET, Ercan N, Krumina G, Rudwan M, et al. Intrathecal gadolinium (gadopentetate dimeglumine) enhanced magnetic resonance myelography and cisternography. Results of a multicenter study. *Invest Radiol.* 2002;37:152-159.
29. Naul LG and Finkenstaedt M. Extensive cerebrospinal fluid enhancement with gadopentetate dimeglumine in a primitive neuroectodermal tumor. *Am J Neurorad* 1997;18:1709–1711
30. Nacar Dogan S, Kizilkilic O, Kocak B, Isler C, et al. (2018). Intrathecal gadolinium-enhanced MR cisternography in patients with otorhinorrhea: 10-year experience of a tertiary referral center. *Neuroradiology.* 2018;60:471-477.
31. Muñoz A, Hinojosa J, Esparza J. Cisternography and Ventriculography Gadopentate Dimeglumine–Enhanced MR Imaging in Pediatric Patients: Preliminary Report. *Am J Neuroradiol.* 2007; 28:889-894
32. Lloyd KM, DelGaudio JM, & Hudgins PA. Imaging of skull base cerebrospinal fluid leaks in adults. *Radiology.* 2008;248:725-736.
33. Zeng QY, Xiong L, Jinkins JR, Liu Z, Fan Z. Intrathecal gadolinium-enhanced MR myelography: a pilot study in human patients (abstr). *Radiology.* 1997;205(P):486.
34. Cebeci H, Bilgin C, Candan S, Demir AB, & Hakyemez, B. Spinal cerebrospinal fluid leakage in spontaneous intracranial hypotension: an intrathecal gadolinium enhanced MR-Myelography study. *J. Belg Soc Radiol.* 2020;104(1)
35. Xie M, Zhou K, Kachra S, McHugh T. et al. Diagnosis and localization of cerebrospinal fluid rhinorrhea: a systematic review. *Am J Rhinol Allerg.* 2022;36:397-406.
36. Yildiz H, Erdogan C, Yalcin R, Yazici Z, et al. Evaluation of communication between intracranial arachnoid cysts and cisterns with phase-contrast cine MR imaging. *Am J Neuroradiol.* 2005;26:145-151.
37. Ray DE, Cavanagh JB, Nolan CC, & Williams S. Neurotoxic effects of gadopentetate dimeglumine: behavioral disturbance and morphology after intracerebroventricular injection in rats. *Am J Neuroradiol.* 1996;17:365-373.
38. Ray DE, Holton JE, Nolan CC, Cavanagh JB, et al. Neurotoxic potential of gadodiamide after injection into the lateral cerebral ventricle of rats. *Am J Neuroradiol.* 1998;19:1455-1462.
39. EL. Jinkins JR, Williams RF, Xiong L. Evaluation of gadopentetate dimeglumine magnetic resonance cisternography in an animal model: preliminary report. *Invest Radiol.* 1999;34:156-159.
40. Algin O, Turkbey B. Intrathecal gadolinium-enhanced MR cisternography: a comprehensive review. *Am J Neuroradiol.* 2013;34:14-22.
41. Morris TW, Ekholm SE, Prentice LJ. The effects of gadolinium- DTPA and DOTA on neural tissue metabolism. *Invest Radiol.* 1991; 26:1087-1090.
42. Provenzano DA, Pellis Z, DeRiggi L. Fatal gadolinium-induced encephalopathy following accidental intrathecal administration: a case report and a comprehensive evidence-based review. *Reg Anesth Pain Med.* 2019;44:721-729. [Published correction appears in *Reg Anesth Pain Med* 2019;44:908.].
43. Samardzic D, Thamburaj K. Magnetic resonance characteristics and susceptibility weighted imaging of the brain in gadolinium encephalopathy. *J Neuroimaging.* 2015;25:136-139.
44. Park KW, Im SB, Kim BT, Hwang SC, et al. Neurotoxic manifestations of an overdose intrathecal injection of gadopentetate dimeglumine. *J Korean Med Sci.* 2010;25:505-508.
45. Martineau, P., Chakraborty, S., Faiz, K., & Shankar, J. Imaging of the spontaneous low cerebrospinal fluid pressure headache: a review. *Canadian Assoc Radiol J.* 2020;71:174-185.
46. Patelb M, Atyani A, Salameh JP, McInnes M, & Chakraborty S. Safety of intrathecal administration of gadolinium-based contrast agents: a systematic review and meta-analysis. *Radiology.* 2020;297:75-83.
47. Evans RW, Armon C, Frohman EM, Goodin DS. Assessment: prevention of post-lumbar puncture headaches: report of the therapeutics and technology assessment subcommittee of the american academy of neurology. *Neurology.* 2000;55:909-914.
48. Woodcock RJ, Marx WF, Johnson RM, Lowe JM, Lipper MH, Kallmes DF. Needle diameter in outpatient myelography: rates of adverse effects and current practice trends. *Neuroradiology.* 2000;42:371-374.
49. Kanda T, Ishii K, Kawaguchi H, Kitajima K, Takenaka D. High signal intensity in the dentate nucleus and globus pallidus on unenhanced T1-weighted MR images: relationship with increasing cumulative dose of a gadolinium-based contrast material. *Radiology* 2014;270:834-841. <https://doi.org/10.1148/radiol.13131669>
50. Gulani V, Calamante F, Shellock FG, Kanal E, Reeder SB. Gadolinium deposition in the brain: summary of evidence and recommendations. *Lancet Neurol* 2017;16:564-570. [https://doi.org/10.1016/s1474-4422\(17\)30158-8](https://doi.org/10.1016/s1474-4422(17)30158-8)

51. Radbruch A, Haase R, Kieslich PJ, Weberling LD, et al. No signal intensity increase in the dentate nucleus on unenhanced T1-weighted MR images after more than 20 serial injections of macrocyclic gadolinium-based contrast agents. *Radiology* 2017;282:699-707. <https://doi.org/10.1148/radiol.2016162241>
52. Ozturk K, Nas OF, Soyly E, Hakyemez B. Signal changes in the Dentate Nucleus and Globus Pallidus on unenhanced T1-weighted Magnetic Resonance Images after intrathecal administration of macrocyclic gadolinium contrast agent. *Invest Radiol.* 2018;53:535-540.
53. Öner AY, Barutcu B, Aykol Ş, Tali ET. Intrathecal contrast-enhanced Magnetic Resonance Imaging-related brain signal changes: Residual gadolinium deposition? *Invest Radiol.* 2017;52:195-197.
54. Edeklev CS, Halvorsen M, Løvland G, Vatnehol SA S, et al. Intrathecal use of gadobutrol for glymphatic MR imaging: prospective safety study of 100 patients. *American Journal of Neuroradiology*, 2019;40:1257-1264.
55. EX. Halvorsen M, Edeklev CS, Fraser-Green J, Løvland G, et al. Off-label intrathecal use of gadobutrol: safety study and comparison of administration protocols. *Neuroradiology.* 2021;63:51-61.
56. Leonetti J, Anderson D, Marzo S, Moynihan G, Siqueira MG, et al. Cerebrospinal fluid fistula after transtemporal skull base surgery. *Otolaryngol Head Neck Surg.* 2001;124:511-514.
57. Dos Santos LR, Cernea CR, Brandao LG. et al. Results and prognostic factors in skull base surgery. *Am J Surg.* 1994;168:481-484.
58. Mendizabal GR, Moreno BC, Flores CC. Cerebrospinal fluid fistula: frequency in head injuries. *Rev Laryngol Otol Rhinol (Bord).* 1992;113:423-425.
59. Bernal-Sprekelsen M, Alobid I, Mullol J, Trobat F, et al. (2005). Closure of cerebrospinal fluid leaks prevents ascending bacterial meningitis. *Rhinology.* 2005;43:277.
60. Reddy M, Baugnon K. Imaging of cerebrospinal fluid rhinorrhea and otorrhea. *Radiol Clin North Am* 2017;55:167-187.
61. Hiremath SB, Gautam AA, Sasindran V, Therakathu J, & Benjamin G. Cerebrospinal fluid rhinorrhea and otorrhea: A multimodality imaging approach. *Diagnostic and Interventional Imaging.* 2019;100:3-15.
62. Aiken AH, Hoots J, Saindane A, et al. Incidence of cerebellar tonsillar ectopia in idiopathic intracranial hypertension: a mimic of the Chiari I malformation. *Am J Neuroradiol.* 2012;33:1901-1906.
63. Constanzo F, Pinto J, Sedaghat S, & Schmidt T. Pseudo-Cerebrospinal fluid leaks of the anterior skull base: algorithm for diagnosis and management. *J of Neurol Surg Part B: Skull Base.* 2021;82:351-356.
64. Vemuri NV, Karanam LS, Manchikanti V, Dandamudi S., et al. Imaging review of cerebrospinal fluid leaks. *Indian Journal of Radiology and Imaging.* 2017;27:441-446.
65. Baker EH, Wood DM, Brennan AL, Baines DL, Phillips BJ. New insights into the glucose oxidase stick test for cerebrospinal fluid rhinorrhoea. *Emerg Med J.* 2005;22:556-557.
66. Zapalac JS, Marple BF, Schwade ND. Skull base cerebrospinal fluid fistulas: a comprehensive diagnostic algorithm. *Otolaryngol Head Neck Surg.* 2002;126: 669-676.
67. De la Peña MJ, Caicoy AG, Rodriguez MR, et al. Spontaneous skull base meningoencephaloceles and cerebrospinal fluid fistulas. *Radiographics.* 2013;33:553-570.
68. Prosser JD, Vender JR, Solares CA. Traumatic cerebrospinal fluid leaks. *Otolaryngol Clin North Am.* 2011;44:857-873.
69. Hiremath SB, Gautam AA, Sasindran V, Therakathu J, & Benjamin G. Cerebrospinal fluid rhinorrhea and otorrhea: A multimodality imaging approach. *Diagnostic and Interventional Imaging.* 2019;100:3-15.
70. Chow JM, Goodman D, Mafee MF. Evaluation of CSF rhinorrhea by computerized tomography with metrizamide. *Otolaryngol Head Neck Surg.* 2003;100:99-105.
71. Ecin G, Oner AY, Tokgoz N, Ucar M, et al. T2-weighted vs. intrathecal contrast-enhanced MR cisternography in the evaluation of CSF rhinorrhea. *Acta Radiol.* 2005;54:698-701.
72. Hatipoğlu HG, Durakoğul T, Ciliz D, Yüksel E. Comparison of FSE T2W and 3D FIESTA sequences in the evaluation of posterior fossa cranial nerves with MR cisternography. *Diagn Interv Radiol.* 2007;13:56-60.
73. Rajeswaran R, Chandrasekharan A, Mohanty S, Murali K, et al. Role of MR cisternography in the diagnosis of cerebrospinal fluid rhinorrhoea with diagnostic nasal endoscopy and surgical correlation. *Indian J Radiol Imaging.* 2006;16:315.
74. Mostafa BE, Khafagi A, & Morcos JJ. Combined HRCT and MRI in the detection of CSF rhinorrhea. *Skull Base.* 2004;14:157-162.
75. Zapalac JS, Marple BF, Schwade ND. Skull base cerebrospinal fluid fistulas: a comprehensive diagnostic algorithm. *Otolaryngol Head Neck Surg.* 2002;126:669-676.
76. Delgaudio JM, Baugnon KL, Wise SK, Patel ZM, et al. Magnetic resonance cisternogram with

- intrathecal gadolinium with delayed imaging for difficult to diagnose cerebrospinal fluid leaks of the anterior skull base. *Int Forum Allergy Rhinol.* 2015;5:333-338.
77. Muñoz A, Martínez-León M, Vázquez É, Pérez da Rosa S, and Crespo J. Intracystic Gadolinium-Enhanced MRI in the Evaluation of Residual Giant-Cystic Craniopharyngiomas in Children: Report of Four Cases. *J Neuroimag.* 2014;24:393-398.
78. Duman, IE, Demerath T, Stadler A, Elsheikh S, et al. High-resolution gadolinium-enhanced MR cisternography using compressed-sensing T1 SPACE technique for detection of intracranial CSF leaks. *Am J Neuroradiol.* 2021;42:116-118.
79. D'Antona L, Merchan MAJ, Vassiliou A, Watkins LD, Davagnanam I, Toma AK, et al.(2021). Clinical presentation, investigation findings, and treatment outcomes of spontaneous intracranial hypotension syndrome: a systematic review and meta-analysis. *JAMA Neurol.* 2021;78:329-337.
80. Arnold M. Headache Classification Committee of the International Headache Society (IHS). The international classification of headache disorders, 3rd edition. *Cephalalgia.* 2018;38:1–211
81. G. Guan J, Couldwell WT, Taussky P. Intracranial hypotension as a complication of lumbar puncture prior to elective aneurysm clipping. *Surg Neurol Int.* 2014;5(Suppl 9):S427–S429.
82. Farnsworth PJ, Madhavan AA, Verdoorn JT, Shlapak JT, Johnson DP, Shlapak DP, et al. Spontaneous intracranial hypotension: updates from diagnosis to treatment. *Neuroradiology.* 2023;233-243.
83. Schrijver I, Schievink WI, Godfrey M, Meyer FB, & Francke U. Spontaneous spinal cerebrospinal fluid leaks and minor skeletal features of Marfan syndrome: a microfibrilopathy. *J Neurosurg.* 2002;96:483-489.
84. Mokri B, Maher CO, Sencakova D. Spontaneous CSF leaks: underlying disorder of connective tissue. *Neurology.* 2002;58:814–816
85. Ferrante, E., Trimboli, M., & Rubino, F. Spontaneous intracranial hypotension: review and expert opinion. *Acta Neurologica Belgica.* 2020;120:9-18.
86. Schievink WI, Maya MM, Jean-Pierre S, Nuño M, Prasad RS, & Moser FG. A classification system of spontaneous spinal CSF leaks. *Neurology.* 2016;87:673-679.
87. Lay CM. Low cerebrospinal fluid pressure headache. *Curr Treat Options Neurol.* 2002;4:357-363.
88. Schievink WI, Maya MM, Louy C, Moser FG, Tourje J. Diagnostic criteria for spontaneous spinal CFS leaks and intracranial hypotension. *Am J Neuroradiol.* 2008;29:853-856.
89. Jones LC, Butteriss D, & Scoffings, D. Spontaneous intracranial hypotension: the role of radiology in diagnosis and management. *Clinical Radiology.* 2021;77:e181-e194.
90. Lin J P, Zhang SD, He FF, Liu MJ, & MaXX. The status of diagnosis and treatment to intracranial hypotension, including SIH. *The Journal of Headache and Pain.* 2017;18:1-8.
91. Kranz PG, Malinzak MD, Amrhein TJ, & Gray L. Update on the diagnosis and treatment of spontaneous intracranial hypotension. *Current pain and headache reports.* 2017;21:1-8.
92. Luetmer PH, Schwartz KM, Eckel LJ, Hunt CH, Carter RE, Diehn FE. When should I do dynamic CT myelography? Predicting fast spinal CSF leaks in patients with spontaneous intracranial hypotension. *Am J Neuroradiol.* 2012;33:690-4. doi:10.3174/ajnr.A2849
93. M, AE. Miyazawa K, Shiga Y, Hasegawa T, Endoh M, Okita N, Higano S, et al. CSF hypovolemia vs intracranial hypotension in "spontaneous intracranial hypotension syndrome". *Neurology.* 2003;60:941–7. doi:10.1212/01.wnl.0000049933.51044.81.
94. Mokri B. Spontaneous cerebrospinal fluid leaks: from intracranial hypotension to cerebrospinal fluid hypovolemia—evolution of a concept. *Mayo Clin Proc.* 1999;74:1113–23. doi:10.4065/74.11.1113
95. Kranz PG, Tanpitukpongse TP, Choudhury KR, Amrhein TJ, Gray L. How common is normal cerebrospinal fluid pressure in spontaneous intracranial hypotension? *Cephalalgia.* 2016; 36: 1209-17.
96. Häni L, Fung C, Jesse CM, Ulrich CT et al. Insights into the natural history of spontaneous intracranial hypotension from infusion testing. *Neurology.* 2020;95:e247-55.
97. Schievink WI, Mokri DW, Mokri B, Silberstein S, Bousser MG, Goadsby PJ. Diagnostic criteria for headache due to spontaneous intracranial hypotension: a perspective. *Headache.* 2011;51:1442-1444. doi:10.1111/j.1526-4610.2011.01911.x
98. Liu FC, Fuh JL, Wang YF, Wang SJ. Connective tissue disorders in patients with spontaneous intracranial hypotension. *Cephalalgia.* 2011;31:691-695. doi:10.1177/0333102410394676
99. Reinstein E, Pariani M, Bannykh S, Rimoin DL, Schievink WI. Connective tissue spectrum

- abnormalities associated with spontaneous cerebrospinal fluid leaks: a prospective study. *Eur J Hum Genet.* 2013;21:386-390. doi:10.1038/ejhg.2012.191
- 100.** Schievink WI. Spontaneous spinal cerebrospinal fluid leaks. *Cephalalgia.* 2008;28:1345-1356.
- 101.** Chen S, Hagiwara M, Roehm P. Spontaneous intracranial hypotension presenting with severe sensorineural hearing loss and headache. *Otol Neurotol.* 2012;33:e65-e66.
- 102.** Schievink WI, Maya MM, Louy C, Moser FG, Sloninsky L. Spontaneous intracranial hypotension in childhood and adolescence. *J Pediatr.* 2013;163:504-510.
- 103.** Capizzano AA, Lai L, Kim J, Rizzo, M et al. Atypical presentations of intracranial hypotension: comparison with classic spontaneous intracranial hypotension. *Am J Neuroradiol.* 2016;37:1256-1261.
- 104.** Tanaka Y, Tosaka M, Fujimaki H, Honda F, Yoshimoto Y. Sex- and age-related differences in the clinical and neuroimaging characteristics of patients with spontaneous intracranial hypotension: a records review. *Headache.* 2016;56:1310-6. doi:10.1111/head.12887
- 105.** Kranz PG, Amrhein TJ, Gray L. CSF venous fistulas in spontaneous intracranial hypotension: imaging characteristics on dynamic and CT myelography. *Am J Roentgenol* 2017;209:1360-66.
- 106.** Takai K, Niimura M, Hongo H, Umekawa M et al. Disturbed consciousness and coma: diagnosis and management of intracranial hypotension caused by a spinal cerebrospinal fluid leak. *World Neurosurg.* 2019;121:e700-e711.
- 107.** Kranz PG, Gray L, Malinzak MD, Amrhein TJ. Spontaneous intracranial hypotension: pathogenesis, diagnosis, and treatment. *Neuroimaging Clin N Am.* 2019; 29:581-594.
- 108.** Schievink WI. Misdiagnosis of spontaneous intracranial hypotension. *Arch Neurol.* 2003;60:1713-1718.
- 109.** Magnaes B. Body position and cerebrospinal fluid pressure. Part 1: clinical studies on the effect of rapid postural changes. *J Neurosurg.* 1976;44:687-97. doi:10.3171/jns.1976.44.6.0687.
- 110.** Schievink WI, Schwartz MS, Maya MM, Moser FG, Rozen TD. Lack of causal association between spontaneous intracranial hypotension and cranial cerebrospinal fluid leaks. *J Neurosurg.* 2012;116:749-54. doi:10.3171/2011.12.JNS111474.
- 111.** Dobrocky T, Mosimann PJ, Zibold F, Mordasini P et al. Cryptogenic cerebrospinal fluid leaks in spontaneous intracranial hypotension: role of dynamic CT myelography. *Radiology.* 2018;289:766-72.
- 112.** Farb RI, Nicholson PJ, Peng PW, Massicotte EM, et al. Spontaneous intracranial hypotension: a systematic imaging approach for CSF leak localization and management based on MRI and digital subtraction myelography. *Am J Neurorad.* 2019;40:745-753.
- 113.** Beck J, Ulrich CT, Fung C, Fichtner J, et al. Diskogenic microspurs as a major cause of intractable spontaneous intracranial hypotension. *Neurology.* 2016;87:1220-6. doi:10.1212/WNL.0000000000003122
- 114.** Yoshida H, Takai K, Taniguchi M. Leakage detection on CT myelography for targeted epidural blood patch in spontaneous cerebrospinal fluid leaks: calcified or ossified spinal lesions ventral to the thecal sac. *J Neurosurg Spine.* 2014;21:3:432-41. doi:10.3171/2014.5.SPINE13549
- 115.** Thielen KR, Sillery JC, Morris JM, Hoxworth JM, et al. Ultrafast dynamic computed tomography myelography for the precise identification of high-flow cerebrospinal fluid leaks caused by spiculated spinal osteophytes. *J Neurosurg Spine.* 2015;22(3):324-31. doi:10.3171/2014.10.SPINE14209
- 116.** Gille O, Soderlund C, Razafimahandri HJ, Mangione P, Vital JM. Analysis of hard thoracic herniated discs: review of 18 cases operated by thoracoscopy. *Eur Spine J.* 2006;15:537-42. doi:10.1007/s00586-005-1014-3
- 117.** Kranz PG, Stinnett SS, Huang KT, Gray L. Spinal meningeal diverticula in spontaneous intracranial hypotension: analysis of prevalence and myelographic appearance. *Am J Neuroradiol.* 2013;34:1284-9. doi:10.3174/ajnr.A3359
- 118.** Sakurai, K., Nishio, M., Yamada, K., Shimohira, et al. Comparison of the radioisotope cisternography findings of spontaneous intracranial hypotension and iatrogenic cerebrospinal fluid leakage focusing on chronological changes. *Cephalalgia.* 2012;32:1131-1139.
- 119.** Schievink WI, Moser FG, & Maya MM. CSF-venous fistula in spontaneous intracranial hypotension. *Neurology.* 2014;83:472-473.
- 120.** Schievink WI, Maya M, Prasad RS, Wadhwa VS, Cruz RB, Moser FG, & Nuno M. Spontaneous spinal cerebrospinal fluid-venous fistulas in patients with orthostatic headaches and normal conventional brain and spine imaging. *Headache: The Journal of Head and Face Pain.* 2021;61:387-391.
- 121.** Kranz PG, Gray L, Malinzak MD, Houk JL, Kim DK, & Amrhein TJ. CSF-venous fistulas: anatomy and diagnostic imaging. *Am J of Roentgenol.* 2021;217:1418-1429.

- 122.** Schievink WI, Moser FG, Maya MM. CSF-venous fistula in spontaneous intracranial hypotension. *Neurology*. 2014;83:472-73.
- 123.** Schievink WI, Moser FG, Maya MM, & Prasad RS. Digital subtraction myelography for the identification of spontaneous spinal CSF-venous fistulas. *J Neurosurg: Spine*. 2016;24:960-964.
- 124.** Luetzen N, Dovi-Akue P, Fung C, Beck J, & Urbach H. Spontaneous intracranial hypotension: diagnostic and therapeutic workup. *Neuroradiology*. 2021;63:1765-1772.
- 125.** Dillon WP. Challenges in the diagnosis and treatment of spontaneous intracranial hypotension. *Radiology*. 2018;289:773-774.
- 126.** Callen AL, Timpone VM, Schwertner A, Zander D. et al. Algorithmic Multimodality Approach to Diagnosis and Treatment of Spinal CSF Leak and Venous Fistula in Patients With Spontaneous Intracranial Hypotension. *Am J Roentgenol*. 2022;219:292-301.
- 127.** Mokri B. The Monro-Kellie hypothesis: applications in CSF volume depletion. *Neurology*. 2001;56:12:1746-1748.
- 128.** Ferrante E, Regna-Gladin C, Arpino I, Rubino F et al. Pseudo-subarachnoid hemorrhage: a potential imaging pitfall associated with spontaneous intracranial hypotension. *Clin Neurol Neurosurg*. 2013;115:2324-2328.
- 129.** Savoirdo M, Minati L, Farina L, Simone T et al. Spontaneous intracranial hypotension with deep brain swelling. *Brain J Neurol*. 2007;130(1):1884-1893. doi:10.1093/brain/awm101
- 130.** Schievink WI, Maya MM, Tourje J & Moser FG, et al. Pseudo-subarachnoid hemorrhage: a CT-finding in spontaneous intracranial hypotension. *Neurology*. 2005;65:135e7. <https://doi.org/10.1212/01.wnl>
- 131.** Dobrocky T, Grunder L, Breiding PS, Brnaca M et al. Assessing spinal cerebrospinal fluid leaks in spontaneous intracranial hypotension with a scoring system based on brain magnetic resonance imaging findings. *JAMA Neurol*. 2019;76:580-587. <https://doi.org/10.1001/jamaneurol.2018.4921>
- 132.** Tosaka M, Sato N, Fujimaki H, Tanaka K et al. Diffuse pachymeningeal hyperintensity and subdural effusion/hematoma detected by fluid-attenuated inversion recovery MR imaging in patients with spontaneous intracranial hypotension. *Am J Neuroradiol*. 2008;29:1164-1170. doi.org/10.3174/ajnr.A1041.
- 133.** Schievink WI, Nuño M, Rozen TD, Maya MM, et al. Hyperprolactinemia due to spontaneous intracranial hypotension. *J Neurosurg*. 2015;122:1020e5. <https://doi.org/10.3171/2014.9.JNS132687>
- 134.** Stone JH, Zen Y, Deshpande V. IgG4-related disease. *N Engl J Med*. 2012;366:539-551.
- 135.** Smith JK, Matheus MG, Castillo M. Imaging manifestations of neurosarcoidosis. *Am J Roentgenol*. 2004;182:289-295.
- 136.** Pickuth D, Spielmann RP, Heywang-Köbrunner SH. Role of radiology in the diagnosis of neurosarcoidosis. *Europ Radiol*. 2000;10:941-944.
- 137.** Fonseka CL, Kanakkahewa TE, Singhapura S, Hewavithana JS et al. Tuberculous pachymeningitis presenting as a diffused dural thickening in a patient with chronic headache and recurrent neurological abnormalities for more than a decade: a case report and a review of the literature. *Case Rep Infect Dis*. 2018.
- 138.** Rosa M Jr, de Almeida Cacador T, Biasutti C, et al. Teaching NeuroImages: skull and dural lesions in neurosyphilis. *Neurology*. 2016;87: e129-30.
- 139.** Bond KM, Benson JC, Cutsforth-Gregory JK, Kim DK, Diehn FE, & Carr CM. Spontaneous intracranial hypotension: atypical radiologic appearances, imaging mimickers, and clinical look-alikes. *Am J Neurorad*. 2020;41:1339-1347.
- 140.** Chen YC, Wang YF, Li JY, Chen SP, et al. Treatment and prognosis of subdural hematoma in patients with spontaneous intracranial hypotension. *Cephalalgia*. 2016;36:225-231.
- 141.** Farb RI, Forghani R, Lee SK, Mikulis DJ, Agid R. The venous distension sign: a diagnostic sign of intracranial hypotension at MR imaging of the brain. *Am J Neuroradiol*. 2007;28(8):1489-93. doi:10.3174/ajnr.A0621
- 142.** Kumar N, Cohen-Gadol AA, Wright RA, Miller M, et al. Superficial siderosis. *Neurology*. 2006;66:1144-1152.
- 143.** Uchino A, Aibe H, Itoh H, Aiko Y, Tanaka M. Superficial siderosis of the central nervous system. Its MRI manifestations. *Clin Imag* 1997;21: 241-245.
- 144.** Webb AJ, Flossmann E, Armstrong RJ. Superficial siderosis following spontaneous intracranial hypotension. *Pract Neurol*. 2015;15:382-384.
- 145.** Wilson, Duncan. Infratentorial superficial siderosis: classification, diagnostic criteria, and rational investigation pathway. *Annals of neurology*. 2017;81: 333-343.
- 146.** Friedauer L, Rezny-Kasprzak B, Steinmetz H, du Mesnil de Rochemont R, & Foerch C. Spinal dural leaks in patients with infratentorial superficial siderosis of the central nervous system-Refinement of a diagnostic algorithm. *Europ J of Neurol*. 2022;29:1136-1144.
- 147.** Koeppen AH, Michael SC, Li D, Chen Z, et al. The pathology of superficial siderosis of the central nervous system. *Acta Neuropathol*. 2008;116: 371-382.

- 148.** Kranz PG, Amrhein TJ, Choudhury KR, Tanpitukpongse TP, Gray L. Time-dependent changes in dural enhancement associated with spontaneous intracranial hypotension. *Am J Roentgenol.* 2016;207:1283-1287. doi:10.2214/AJR.16.16381
- 149.** Schievink WI. Spontaneous spinal cerebrospinal fluid leaks and intracranial hypotension. *JAMA.* 2006;295:2286-96. doi:10.1001/jama.295.19.2286
- 150.** Spelle L, Boulin A, Pierot L, et al. Spontaneous intracranial hypotension: MRI and radionuclide cisternography findings. *J Neurol Neurosurg Psychiatry.* 1997;62:291-292.
- 151.** CF.Sehgal AK, Sethi RS, Raghavan S, & Namgyal PA. Radionuclide cisternography: a prudent investigation in diagnosing spontaneous intracranial hypotension. *Indian J Nucl Med.* 2013;28:42-44.
- 152.** Sakurai, M. Nishio, S. Sasaki, H. Ogino, J. Tohyama, K. Yamada, Y. Shibamoto Postpuncture CSF leakage: a potential pitfall of radionuclide cisternography. *Neurology.* 2010;75:1730-1734.
- 153.** Wang YF, Fuh JL, Lirng JF, Chen SP, Hseu SS, Wu JC, Wang SJ. Cerebrospinal fluid leakage and headache after lumbar puncture: a prospective non-invasive imaging study. *Brain.* 2015;138:1492-1498.
- 154.** Evangelou P, Omrane MA, Thurow J, Mix M, et al. 68Ga-DOTA Positron Emission Tomography for Diagnosis of Spinal Cerebrospinal Fluid Leaks. *J Nuclear Med.* 2022;122.264059; DOI: <https://doi.org/10.2967/jnumed.122.264059>
- 155.** Tomoda Y, Korogi T, Aoki T, Morioka, et al. Detection of cerebrospinal fluid leakage: initial experience with three-dimensional fast spin-echo magnetic resonance myelography. *Acta Radiol.* 2008;49:197-203.
- 156.** Watanabe A, Horikoshi T, Uchida M, Koizumi H, et al. Diagnostic value of spinal MR imaging in spontaneous intracranial hypotension syndrome. *Am J Neuroradiol.* 2009;30:147-151.
- 157.** Schievink WI, Maya MM, Tourje J. False localizing sign of C1e2 cerebrospinal fluid leak in spontaneous intracranial hypotension. *J Neurosurg.* 2004;100:639-644. <https://doi.org/10.3171/jns.2004.100.4.0639>
- 158.** Dobrocky T, Winklehner A, Breiding PS, Grunder L, et al. Spine MRI in Spontaneous Intracranial Hypotension for CSF Leak Detection: Nonsuperiority of Intrathecal Gadolinium to Heavily T2-Weighted Fat-Saturated Sequences. *Am J Neuroradiol.* 2020;41:1309-1315.
- 159.** Piechowiak El, Pospieszny K, Haeni L, Jesse CM, et al. Role of conventional dynamic myelography for detection of high-flow cerebrospinal fluid leaks: optimizing the technique. *Clinical Neurorad.* 2021;31:633-641.
- 160.** Ferrante E, Rubino F, Beretta F, Regna-Gladin, & Ferrante MM. Treatment and outcome of subdural hematoma in patients with spontaneous intracranial hypotension: a report of 35 cases. *Acta Neurol Belg.* 2018;118:61-1170.
- 161.** Maus T, Schueler BA, Leng S, Magnuson D, et al. Radiation dose incurred in the exclusion of vascular filling in transforaminal epidural steroid injections: fluoroscopy, digital subtraction angiography, and CT/fluoroscopy. *Pain Med.* 2014;15:1328-1333.
- 162.** Houk JL, Marin DM, Malinzak MD, Kranz PG, & Amrhein T J. Dual energy CT for the identification of CSF-venous fistulas and CSF leaks in spontaneous intracranial hypotension: report of four cases. *Radiology Case Reports.* 2022;17:1824-1829.
- 163.** Schievink WI, Maya MM, Moser F, Prasad R, et al. Multiple spinal CSF leaks in spontaneous intracranial hypotension: do they exist?. *Neurology: Clinical Practice.* 2021;11:e691-e697.
- 164.** Amrhein TJ, Gray L, Malinzak MD, & Kranz PG. Respiratory phase affects the conspicuity of CSF-venous fistulas in spontaneous intracranial hypotension. *Am J Neuroradiol.* 2020;41:1754e6. <https://doi.org/10.3174/ajnr.A6663>.
- 165.** Kinsman KA, Verdoorn JT, Luetmer PH PH, Clark MS, & Diehn FE. Renal contrast medium on CT myelography: diagnostic value in patients with spontaneous intracranial hypotension. *Am J Neuroradiol.* 2019;40:376e81. <https://doi.org/10.3174/ajnr.A5934>
- 166.** Kranz PG, Gray L, Malinzak MD, Houk, JL, Kim, DK & Amrhein TJ. CSF-venous fistulas: anatomy and diagnostic imaging. *Am J Roentgenol.* 2021;217:1418e29. <https://doi.org/10.2214/AJR.21.26182>
- 167.** Schievink WI, Maya MM, Moser FG, Prasad, RS, et al. Lateral decubitus digital subtraction myelography to identify spinal CSF-venous fistulas in spontaneous intracranial hypotension. *J Neurosurg Spine.* 2019; 31: 902-05.
- 168.** Mamlouk MD, Ochi RP, Jun P, Shen PY. Decubitus CT myelography for CSF-venous fistulas: a procedural approach. *Am J Neuroradiol.* 2021; 42:32-36.
- 169.** Kim DK, Brinjikji W, Morris PP, Diehn PP, et al. Lateral decubitus digital subtraction myelography: tips, tricks, and pitfalls. *Am J Neuroradiol.* 2020; 41: 21-28.
- 170.** Caton MT, Laguna B, Soderlund KA, Dillon WP, Shah VN. Spinal compliance curves: preliminary experience with a new tool for evaluating suspected CSF venous fistulas on CT myelography in

- patients with spontaneous intracranial hypotension. *Am J Neuroradiol.* 2021; 42:986-992.
- 171.** Clark MS, Diehn FE, Verdoorn JT, Lehman VT, et al. Prevalence of hyperdense paraspinal vein sign in patients with spontaneous intracranial hypotension without dural CSF leak on standard CT myelography. *Diagn Interv Radiol.* 2018;24:54-59.
- 172.** Kranz PG, Amrhein TJ, Schievink WI, Karikari IO, et al The “hyperdense paraspinal vein” sign: a marker of CSF-venous fistula. *Am J Neuroradiol.* 2016;37:1379–1381
- 173.** Behbahani S, Raseman J, Orlowski H, Sharma A, Eldaya R. Renal excretion of contrast on CT myelography: a specific marker of CSF leak. *Am J Neu*
- 174.** Kinsman KA, Verdoorn JT, Luetmer PH, Clark MS, Diehn FE. Renal contrast on CT myelography: diagnostic value in patients with spontaneous intracranial hypotension. *Am J Neuroradiol.* 2019;40: 376-81.
- 175.** Hattingen E, DuMesnil R, Pilatus U, Raabe A, T. et al. Contrast-enhanced MR myelography in spontaneous intracranial hypotension: description of an artefact imitating CSF leakage. *Eur Radiol.* 2009;19:1799-1808.
- 176.** Williams EC, Buchbinder BR, Ahmed S, Alston TA, et al. Spontaneous intracranial hypotension: presentation, diagnosis, and treatment. *Anesthesiology.* 2014;121:1327-33.
- 177.** Chazen JL, Talbott JF, Lantos JE, Dillon WP. MR myelography for identification of spinal CSF leak in spontaneous intracranial hypotension. *Am J Neuroradiol.* 2014;35:2007-2012.
- 178.** Akbar J, Luetmer PH, Schwartz K, Hunt C, et al. The role of MR myelography with intrathecal gadolinium in localization of spinal CSF leaks in patients with spontaneous intracranial hypotension. *Am J Neuroradiol.* 2012;33:35–540. DOI: 10.3174/ajnr.A2815
- 179.** Albes G, Weng H, Horvath D, Musahl C, et al. Detection and treatment of spinal CSF leaks in idiopathic intracranial hypotension. *Neuroradiology.* 2012;54:1367–73. DOI: 10.1007/s00234-012-1055-1053.
- 180.** Graff-Radford SB, Schievink WI. High-pressure headaches, low pressure syndromes, and CSF leaks: diagnosis and management. *Headache.* 2014;54:394-401.
- 181.** Griauzde J, Gemmete JJ, Pandey AS, Chaudhary N. Intrathecal preservative-free normal saline challenge magnetic resonance myelography for the identification of cerebrospinal fluid leaks in spontaneous intracranial hypotension. *J Neurosurg.* 2015;123:732-736.
- 182.** Tyagi A. Management of spontaneous intracranial hypotension. *Pract Neurol.* 2016;16:87-88.
- 183.** GE. Sudlow C, Warlow C. Epidural blood patching for preventing and treating post-dural puncture headache. *Cochrane Database Syst Rev.* 2010(1).